



UNITED NATIONS
UNIVERSITY
UNU-WIDER

WIDER Working Paper 2014/121

Planning for large-scale wind and solar power in South Africa

Identifying cost-effective deployment strategies through spatiotemporal modelling

Kevin Ummel¹ and Charles Fant²

October 2014

Abstract: South Africa hopes to expand wind and solar power. Success depends on how and where to deploy the technologies. This study develops a 10-year database of expected power generation for these technologies across South Africa. A power system model simulates the performance of different spatial deployment strategies in 2040. The results suggest that optimization of the location and quantities of the technologies could significantly reduce the cost of greenhouse gas abatement compared to conventional approaches. The data and techniques utilize open-source satellite data and software to minimize the cost of analysis, an approach that could be translated to other contexts.

Keywords: abatement cost, greenhouse gas emissions, low-carbon development, optimization, renewable energy, spatiotemporal modelling

JEL classification: Q40, Q42, Q47

Acknowledgements: This analysis was funded by the Center for Global Development (CGD). The authors are grateful for support of this work from the board of directors and funders of CGD, including the Royal Danish Embassy.

¹Center for Global Development, kevinummel@gmail.com; ²Massachusetts Institute of Technology, chasfant@mit.edu

This study has been prepared within the UNU-WIDER project on Development under Climate Change, directed by Channing Arndt, James Thurlow, and Finn Tarp.

Copyright © UNU-WIDER 2014

ISSN 1798-7237 ISBN 978-92-9230-842-1 <https://doi.org/10.35188/UNU-WIDER/2014/842-1>

Typescript prepared by Sophie Richmond for UNU-WIDER.

UNU-WIDER gratefully acknowledges the financial contributions to the research programme from the governments of Denmark, Finland, Sweden, and the United Kingdom.

The World Institute for Development Economics Research (WIDER) was established by the United Nations University (UNU) as its first research and training centre and started work in Helsinki, Finland in 1985. The Institute undertakes applied research and policy analysis on structural changes affecting the developing and transitional economies, provides a forum for the advocacy of policies leading to robust, equitable and environmentally sustainable growth, and promotes capacity strengthening and training in the field of economic and social policy-making. Work is carried out by staff researchers and visiting scholars in Helsinki and through networks of collaborating scholars and institutions around the world.

UNU-WIDER, Katajanokanlaituri 6 B, 00160 Helsinki, Finland, wider.unu.edu

The views expressed in this publication are those of the author(s). Publication does not imply endorsement by the Institute or the United Nations University, nor by the programme/project sponsors, of any of the views expressed.

1 Introduction

Over 135 countries have adopted renewable energy deployment targets, with particular focus on harnessing wind and solar energy for electricity production (REN21 2013). South Africa's aspirations are particularly noteworthy given its heavy reliance on coal, which supplies more than 90 per cent of the country's electricity. The government's integrated resource plan (IRP) for the power sector, approved in 2011, slates wind and solar power (WSP) to provide 21 per cent of generating capacity by 2030 (DOE 2011). Planning scenarios developed by the state-owned utility Eskom envision WSP penetration potentially reaching 40 per cent by 2040 (Eskom 2012).

Estimations of wind potential in South Africa have varied from 7.9 TWh (terawatt hours) (Diab 1985) to 106 TWh (Banks and Schäffler 2007). Note that the more recent studies estimate higher wind power potential than the older studies. This pattern of increased estimates persisted from 1985 to 2007. The most detailed estimate comes from Hagemann (2008), who estimated South Africa's generation potential to be: 80.54 TWh with a realistic estimation, 157.18 with an optimistic estimation, and 20.06 TWh with a pessimistic estimation. Solar potential is estimated to be much higher than wind potential in South Africa, although there are fewer estimates in the literature. The most recent estimate found is included in Fluri (2009), who estimates concentrating solar power (CSP) potential to be 547.6 GW (gigawatt), producing about 1,861 TWh annually. The majority of this potential is in the Northern Cape, with an estimated potential of 510.3 GW.

While WSP offers many socioeconomic and environmental benefits, it also introduces unique challenges. Wind and solar resources vary significantly across space and time; WSP is inherently intermittent (Hansen 1998; Peterson et al. 1997). There are many ways to mitigate this intermittency as presented by Delucchi and Jacobson (2011). The most accessible, and often the cheapest option for control over the magnitude and timing of WSP generation is in the siting of projects across space. Once a project is constructed, weather patterns dictate performance.

In contrast, the magnitude and timing of conventional generation is controlled by plant operators; fossil fuel generators are highly dispatchable. Replacing dispatchable generation with intermittent WSP, as power sectors around the world hope to do, makes it more difficult to ensure that power is available when needed. The reliability and cost of power systems with high penetration of WSP are determined by the nature of wind and solar resources in the region, the way in which WSP technologies are distributed across space, and the ability of conventional generators to accommodate intermittency.

South Africa and other countries face a common challenge: how to turn laudable renewable power aspirations into concrete plans. This is an exceptionally complex task, and it hinges largely on the question of how and where to deploy WSP. Well-designed deployment strategies can take advantage of natural variability in WSP resources across space and time to minimize costs and maximize benefits, while ensuring reliability. Poor deployment strategies risk locking countries into multi-decade infrastructure investments that unnecessarily increase the cost of electricity.

Given the tremendous complexity and long-time horizons involved, robust data and modelling techniques are needed to inform power sector planning and project procurement. Existing investment allocation models like MARKAL (Fishbone and Abilock 1981) or BALMOREL (as demonstrated in Ball et al. 2007) have been around for decades. These models, which were originally designed for conventional energy investment, model energy investment evolution over 40 to 50 years, using representative time slices (e.g. weekend-night) for expected power supply. The main differences between the modelling in this study and these existing investment planning

models is that (1) we simplify the model by focusing decisions on WSP investment whereas the preceding models allow investment in all energy generating types, (2) we model the system at a snapshot in 2040, rather than the investment progression over time and (3) we model at an hourly time-step for 10 years with consecutive realistic generation estimates rather than using representative time slices. Differences (1) and (2) are simplifications used in this study, but are not necessary. The main contribution to the current body of literature is (3), which is more important for modelling WSP than for conventional supply because of the intermittency associated with WSP generation; traditional capacity estimates do not address the risk of intermittency (Gunturu and Schlosser 2012; Philbrick 2011). For this reason, the use of multi-year, hourly time series is critical to accurate calculation of long-term reliability of intermittent sources. In an analysis of high-resolution wind power data from Ireland, Hasche et al. (2011) show that at least five years of hourly data (and ideally more) are needed to accurately calculate the ability of the wind power fleet to contribute to system adequacy. Longer time series, such as the ten years of hourly data used here, capture the considerable inter-annual variability that shorter time series miss.

A number of studies have assessed the value of wind and solar site interconnection using a consecutive hourly to sub-hourly time-step (among others, Elhadidy 2000; Reichling and Kulacki 2007). These studies analyse the benefits of connecting a few sites in a study region, less than 20, and over short periods, one to two years. These studies provide insight into the techniques used to assess small-scale interconnection possibilities and benefit from site simplicity but provide less insight into national-scale wind and solar build-out targets. On the other hand, a number of studies have assessed large-scale penetration of wind and solar technologies; most also include biomass and hydropower: among others, Parsons-Brinckerhoff (2009) for the UK; Pricewaterhouse-Coopers et al. (2010) for Europe and North Africa; Alliance for Climate Protection (2009) for the United States; and Jacobson and Delucchi (2011) for the globe. These studies present technically feasible energy build-out targets where either the majority (greater than 80 per cent) or all power is generated with renewable energy. While these exercises are useful optimistic goals, they are not likely to become a reality in coming decades, restricted by a lack of realistic political and/or economic support.

This study addresses the case of South Africa in two ways: First, expected generating efficiency for key WSP technologies is modelled at hourly resolution over a 10-year period across the country. Second, a simple power system model is used to simulate the economic and environmental performance of different WSP deployment scenarios in the year 2040. The basic objective is to demonstrate the ability of low-cost data and modelling techniques to capture the spatiotemporal dynamics critical to power systems with high penetration of WSP and to quantify the potential savings from better long-term planning.¹

Section 2 describes the development of a 10-year, hourly resolution database of wind speed, solar radiation, and general meteorological conditions for South Africa. Section 3 describes how the physical resource data are used to model the expected hourly performance of onshore wind farms, utility-scale photovoltaic (PV), and CSP facilities. Section 4 summarizes observed spatiotemporal patterns in WSP generating efficiency. Section 5 describes the creation of projected hourly load data for 2040. Section 6 describes the development of a simple power system model and WSP deployment scenarios for 2040. Section 7 presents simulation results for those scenarios. Section 8 discusses the results and potential for spatiotemporal modelling to improve WSP deployment outcomes and project procurement in South Africa and other countries.

¹ This work was also published as a working paper through the Center for Global Development (Ummel 2013).

2 Wind and solar resource data

Modelling of WSP technologies requires numerous data inputs, ideally at high spatial and temporal resolution. This section describes the creation of hourly resource variables over a 10-year period at 0.125° spatial resolution by combining output from NASA’s Goddard Earth Observing System (GEOS-5) climate model with surface solar irradiance data from the Climate Monitoring Satellite Application Facility (CM-SAF) and data produced by the Wind Atlas for South Africa (WASA) project.² The resulting data include global and diffuse horizontal irradiance, direct normal irradiance, wind speed at 10 m and 100 m above ground level (a.g.l.), and additional ‘secondary’ variables like wind direction, ambient temperature, relative humidity, air pressure, and surface albedo.

2.1 Wind speed

High-resolution wind speed datasets from numerical weather modelling are commercially available but typically cost-prohibitive for large-scale analysis. The approach described below combines output from NASA’s GEOS-5 climate model with data from the numerical wind atlas produced by the WASA project. Together, these data allow the generation of plausible hub-height hourly wind speed time series for the period 1996 through 2005 for a region in the south-west of the country covering the majority of the documented wind potential, including most of the Western Cape and parts of the Northern and Eastern Cape provinces.

NASA’s Modern Era Retrospective Analysis for Research and Applications (MERRA) project utilizes the GEOS-5 climate model to produce a global assimilation and re-analysis of the satellite and surface record from 1979 to present (Rienecker et al. 2008). MERRA/GEOS-5 (version 5.2) provides the highest-resolution global reanalysis output currently available and provides boundary conditions for operational weather forecasts and higher-resolution numerical weather models.

Initial estimates of hourly wind speed at 10 m and 100 m a.g.l. are created using surface friction velocity from GEOS-5 in conjunction with the logarithmic wind profile, assuming neutral stability. Gunturu and Schlosser (2012) use the same data and technique in their analysis of wind power resources in the United States. Surface friction velocity at the native GEOS resolution is bilinearly downscaled to the 0.125° resolution and the logarithmic profile applied (Eq. 1).

$$V_z = \frac{u_s}{k} \left[\log \left(\frac{z-d}{z_0} \right) \right] \quad (1)$$

V_z is the horizontal wind velocity at height z above ground level, u_s is the surface friction velocity, k is the von Karman constant (0.41), d is the displacement height, and z_0 is the roughness length.

The surface roughness data are constructed from the United States Geological Survey (USGS) Global Land Cover Characteristics v2.0 database³ with a native resolution of $\sim 0.01^\circ$, using a land-cover-to-surface roughness look-up table provided by the WASA project. Displacement height is assumed to be two-thirds of the mean vegetation height, as given by Simard et al. (2011) at a native resolution of $\sim 0.01^\circ$.

The coarse spatial resolution of the GEOS-5 model does not sufficiently capture small-scale wind patterns driven by microclimates and local orography. The WASA project has generated a high-resolution (~ 5 km) climatological wind speed database for a region covering the south-west of the

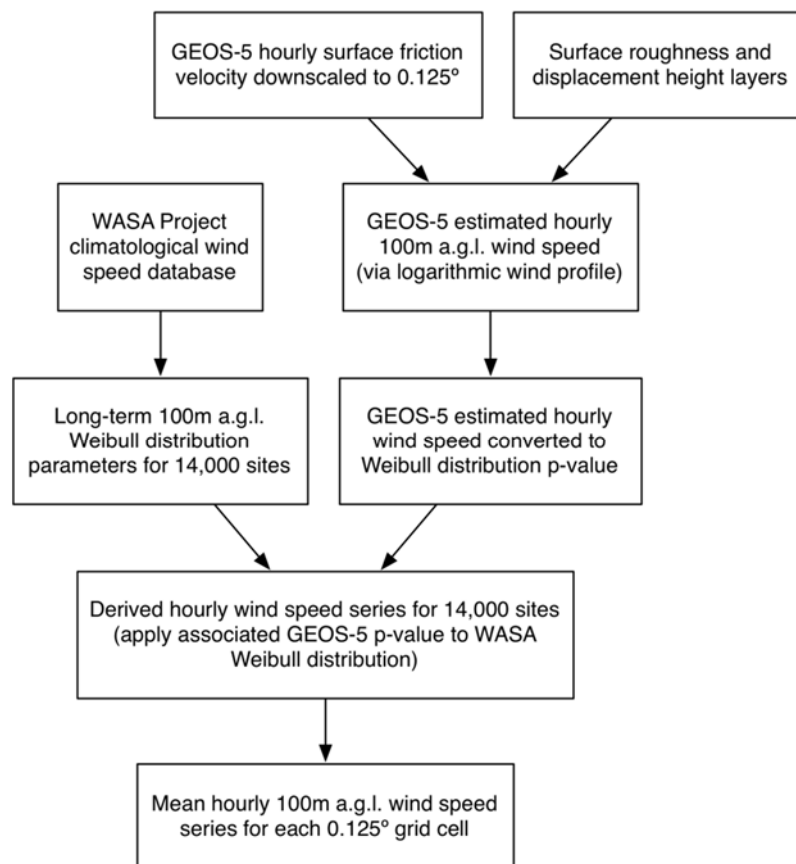
² See: www.wasaproject.info

³ See: http://edc2.usgs.gov/glcc/globe_int.php

country. This wind atlas better reflects local terrain but (to date) only provides the long-term wind speed distribution at various heights for a given site, not hourly time series.

Estimated hourly wind speed data from GEOS-5 and wind speed distribution data from WASA are combined to create hub-height (100 m a.g.l.) time series. The WASA data are processed to extract long-term Weibull distribution parameters describing the expected wind speed distribution at ~14,000 sites. For each 0.125° downscaled MERRA grid cell, a Weibull distribution is fitted to the GEOS-5 100 m a.g.l. hourly wind speed and each observation converted to its distribution p-value. Next, for each WASA site within a given grid cell, the p-values are translated to hourly mean wind speed using the Weibull distribution provided by WASA. The resulting time series are averaged to produce a single, long-term hourly time series for each 0.125° grid cell. Figure 1 illustrates the data processing chain.

Figure 1: Wind speed series (100 m a.g.l.) processing chain



Source: Authors' creation.

2.2 Solar radiation

Surface solar radiation data are provided by CM-SAF and include both global and direct mean hourly irradiance on a horizontal surface. The data result from processing the first-generation Meteosat satellite record from 1983 to 2005 (Mueller et al. 2012; Posselt et al. 2012). Three satellite observations are used to construct each hourly mean. The processing algorithm uses effective cloud albedo to estimate cloud transmissivity when calculating irradiance at the surface.

Hourly data were obtained for the period 1 January 1996 through 31 December 2005 for all of South Africa. Though available at a native spatial resolution 0.03°, mean irradiance was extracted at 0.125° resolution to reduce computational demands. Global and direct horizontal irradiance, in

conjunction with standard astronomical position algorithms, were used to calculate hourly direct normal irradiance (DNI). The 10-year record was also processed to determine the maximum hourly ‘DNI-cosine product’ for each grid cell, using equations and assumptions of Wagner and Gilman (2011). This quantity is critical to specifying the solar field design parameters of CSP systems (see Section 3).⁴

2.3 Secondary variables

Additional variables were extracted from GEOS-5 model output, including ambient air temperature, specific humidity, surface air pressure, wind direction, and surface albedo. All were bilinearly downscaled to 0.125° resolution. Temperature and pressure were additionally adjusted for local elevation using standard environmental lapse rates. These variables and standard meteorological formulae allow the calculation of additional quantities (e.g. relative humidity, dew-point temperature) necessary for accurate modelling of generating efficiency (see Section 3).

3 Modelling WSP generating efficiency

The physical resource time series serve as inputs to the National Renewable Energy Laboratory’s System Advisor Model (SAM) software, allowing hourly simulation of generating efficiency for hypothetical PV, CSP, and wind farm installations. This section describes the chosen SAM system parameters for each technology. Simulations were conducted with SAM software v2013.1.15 (Gilman and Dobos 2012; SAM 2013). A full 10 years of hourly meteorological data (including ‘secondary variables’ described above) are used as inputs to SAM, resulting in 10-year hourly generating efficiency time series.

It is not necessary (nor computationally convenient) to model hourly efficiency for *every* grid cell. Instead, for each WSP technology a subset of grid cells is selected. The SKATER spatial clustering algorithm is used to segment grid cells into contiguous clusters of a minimum size (2,500 km² for wind and 5,000 km² for PV and CSP), with clusters selected so they contain resource time series that have similar diurnal profiles over each season (Lage et al. 2001).

That is, the primary physical resource time series for wind, PV, and CSP technologies (hub-height wind speed, global horizontal irradiance [GHI], and DNI, respectively) are used to cluster grid cells in a way that distinguishes between areas with different temporal resource regimes. Within each cluster returned by SKATER, the grid cell with the highest mean annual resource value is then chosen for modelling in SAM. This technique reduces computational demands, while ensuring that the sampled sites capture the range of spatiotemporal diversity in the full dataset.

3.1 Onshore wind power

The wind farm model assumes a 100 MW array consisting of 50 Vesta v90 2.0 MW turbines with 100 m hub height and 90 m rotor diameter. The turbines are laid out in a 5×10 rectangular field, with downstream and transverse turbine spacing equal to 10 and 5 rotor diameters, respectively. For each simulated site, the array is oriented so that the downstream spacing is parallel to the predominant wind direction observed over the 10-year wind speed time series in order to more

⁴ There are occasional gaps in the CM-SAF radiation data, typically about two days per year. Missing data are replaced with the mean value for the same hour over the preceding and proceeding five days. The one exception is an extended period of missing direct horizontal irradiance data from 9 June 1997 to 30 June 1997. Replacement values are generated by calculating the hourly ratio of direct to global horizontal irradiance for the same period in 1998 and then applying the ratios to observed hourly global horizontal irradiance in 1997.

accurately capture losses due to wake effects. All other variables are set to SAM default values. Turbine and array performance are simulated using the wind farm model of Quinlan (1996).

3.2 Photovoltaic power

The PV model assumes the use of 230 Jinko Solar JKM230M-60B monocrystalline modules in conjunction with SMA Solar SB10000TL inverters. The modules are ground-mounted on single-axis east–west tracking arrays utilizing a backtracking algorithm and maximum rotation of +/- 60 degrees. Array spacing assumes a ground cover ratio of 0:4. All other variables are set to SAM default values. Module performance is simulated using the California Energy Commission (CEC) model and associated module characteristics database (De Soto 2004; Dobos 2012). Temperature correction is provided by the nominal operating cell temperature (NOCT) model of Neises (2011). Inverter performance is simulated using the Sandia National Laboratories model of King et al. (2007) and associated inverter database.

3.3 Concentrating solar power

The CSP model assumes a 100 MW_{net} facility with parabolic trough collector technology, air-cooled condensers, and six hours of molten salt storage capability. The IRP includes cost assumptions for CSP facilities with zero, three, six, and nine hours of thermal storage. Six hours was chosen as a middle-of-the-road value. In practice, the amount of storage is likely to vary across facilities. It is expected that air-cooled condensers will be preferred in water-scarce areas.

For each simulated site, the solar field is sized to provide a solar multiple of 2.5 at the design irradiance point, with the latter equal to the maximum hourly DNI-cosine product calculated over the entire 10-year time series. Variables other than those discussed below are set to SAM default values. System performance is simulated using the physical trough model of Wagner and Gilman (2011).

Because CSP systems (and especially those with storage capability) exhibit thermal inertia, generating efficiency in a given hour can be controlled, to some degree, by the plant operator. This unique behaviour is most relevant during periods of high electricity demand, when system and plant operators may wish to curtail generation in the hours preceding peak demand in order to charge the storage system and allow maximum electricity generation when it is needed most (for example, in the evening after the sun has set).

In practice, optimal or near-optimal behaviour of this kind is determined endogenously and dictated by complex, real-time power system considerations, weather forecasts, electricity prices, etc. The parameters guiding SAM's internal CSP plant control algorithm (which decides when to direct energy to the generator block versus storage) are adjusted in an attempt to approximate such behaviour exogenously.

Projected electricity demand, operating costs, generating fleet characteristics, and representative wind and PV generating efficiency time series are used to estimate marginal running costs (i.e. per unit revenue in a competitive electricity market) that might confront South African CSP operators for various hours of the year in 2040 (per the scenarios described in Section 6). High marginal running costs indicate hours when the generating fleet is operating near capacity and additional generation (provided by CSP plants) is highly valued. In South Africa, this primarily occurs during winter evenings (see Section 5).

This information was introduced into SAM's thermal storage dispatch schedule and, for a small set of representative locations, the parameters guiding plant operation were optimized to find those

that minimized the levelized cost of electricity. Those parameters were then applied universally when simulating the performance of other sites. The net result is suppressed CSP generation during winter afternoons in order to provide maximum output during the evening. Outside of winter (May–August), the default plant control algorithm is used.

4 Spatiotemporal patterns in expected generating efficiency

The SAM simulations result in 10-year hourly generating efficiency time series for 176 PV sites, 178 CSP sites, and 110 wind farm sites. This section summarizes the spatial and temporal patterns observed in those data.

The term ‘generating efficiency’ is used here to specify mean hourly power output as a fraction of net generating capacity. It is synonymous with ‘hourly capacity factor’. A generating efficiency of one indicates the technology is capable of operating at maximum capacity during the hour.

The WSP generating efficiency time series analysed in this section are available to the public per the Center for Global Development’s data disclosure policy. Data files and sample code can be downloaded from the website.⁵

4.1 Exclusion of areas deemed infeasible

The maps below exclude areas (indicated by white grid cells) that are considered infeasible for siting of facilities. The exclusion screens are from Ummel (2011), which provides high-resolution WSP screens at global scale built from a range of geospatial data layers. The technology-specific screens consider land cover, terrain slope, proximity to human populations, geomorphology, and protected areas and parks.

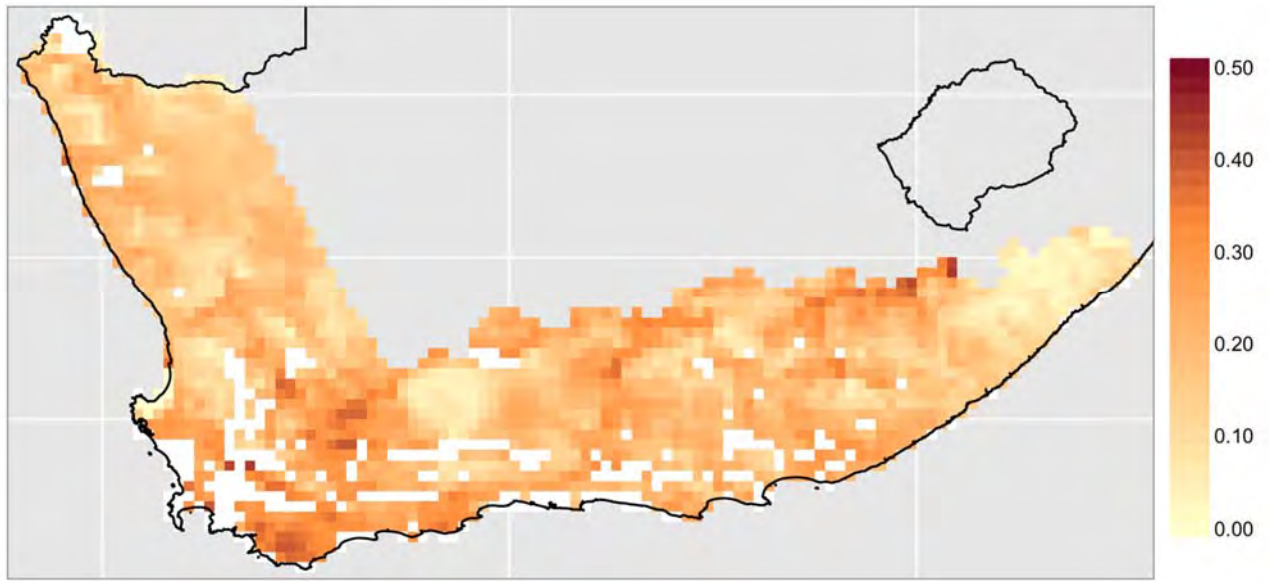
4.2 Long-term mean efficiency across space

In the interest of providing long-term mean generating efficiency maps, the 10-year time series results were averaged over the full period for each modelled grid cell and technology. The results were then spatially interpolated for non-modelled grid cells using a combination of universal kriging and an automatic variogram fitting procedure (Hiemstra et al. 2009). For each technology, the kriging model includes an observed variable in addition to location. For wind, the predictor is mean hourly hub-height wind speed converted to generating efficiency via a generic wind turbine power curve. Mean hourly GHI and DNI are used for PV and CSP, respectively.

Long-term wind farm generating efficiency (100 m hub height) reaches up to 50 per cent in the most suitable locales (Figure 2). The extent of the study area is restricted to the area covered by the WASA numerical wind atlas. The most efficient locales cluster in the Western Cape, to the north-east and south-east of Cape Town, and in the northern reaches of the Eastern Cape. There is also evidence of strong, but spatially limited, potential among coastal sites in the Northern Cape.

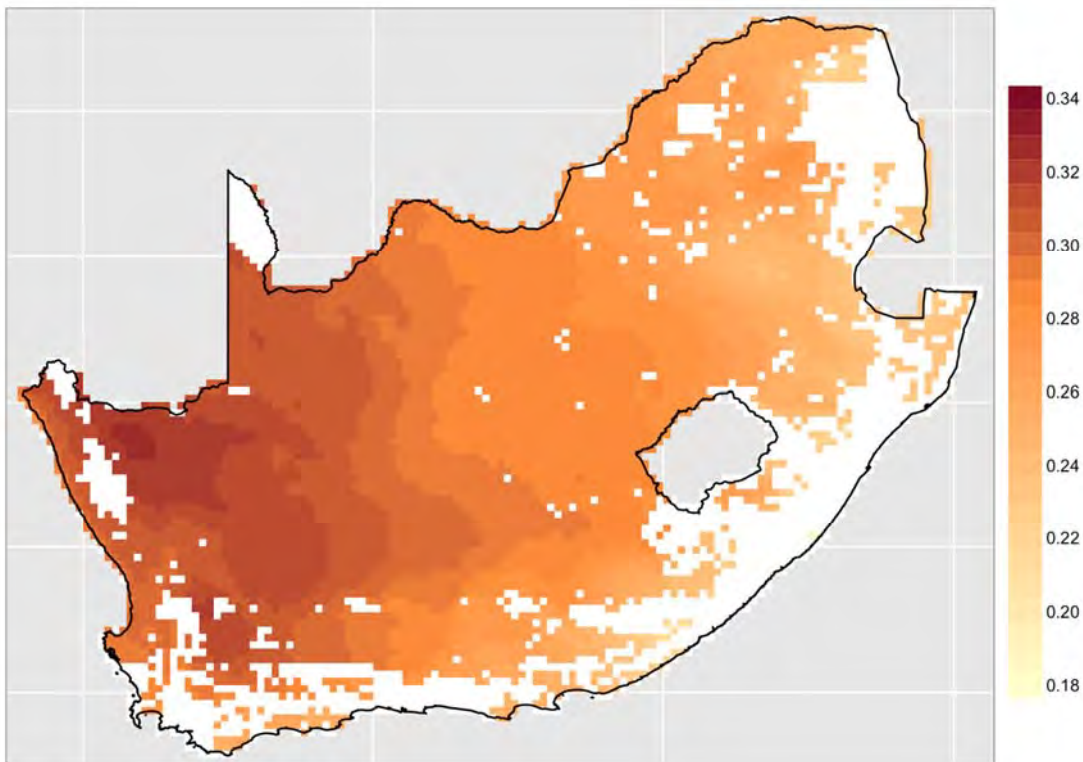
⁵ See: <http://www.cgdev.org/page/research-data-and-code-disclosure> and [http://www.cgdev.org/section/publications?f\[0\]=field_document_type%3A2057](http://www.cgdev.org/section/publications?f[0]=field_document_type%3A2057)

Figure 2: Mean modelled wind farm (100 m hub height) generating efficiency (1996–2005)



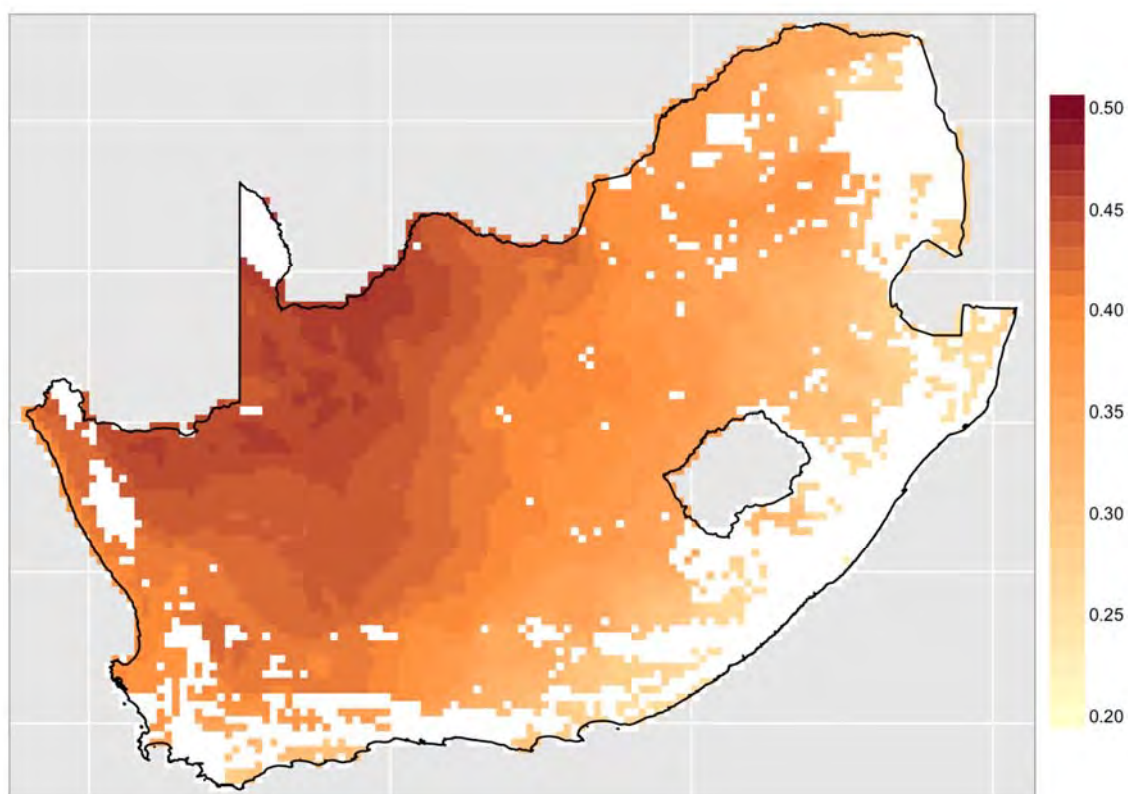
Source: Authors' creation (data modelled by SAM).

Figure 3: Mean modelled utility-scale PV (monocrystalline) generating efficiency (1996–2005)



Source: Authors' creation (data modelled by SAM).

Figure 4: Mean modelled CSP (6-hour storage; air-cooled) generating efficiency (1996–2005)



Source: Authors' creation (data modelled by SAM).

It is important to mention that the wind farm exclusion screen specifically excludes cropland. Although wind turbines can be placed on agricultural land, conversations with Eskom staff indicated likely resistance to wind farm development among agricultural interests in South Africa. Some areas with good wind resources are consequently excluded from Figure 2 and the subsequent analysis.

Long-term PV generating efficiency exceeds 30 per cent in the highest-efficiency sites in the Northern Cape (Figure 3). The best sites are located significantly to the west, with some high-quality locales stretching south into the Western Cape. There are moderate PV resources in the north-east around the Pretoria/Johannesburg area.

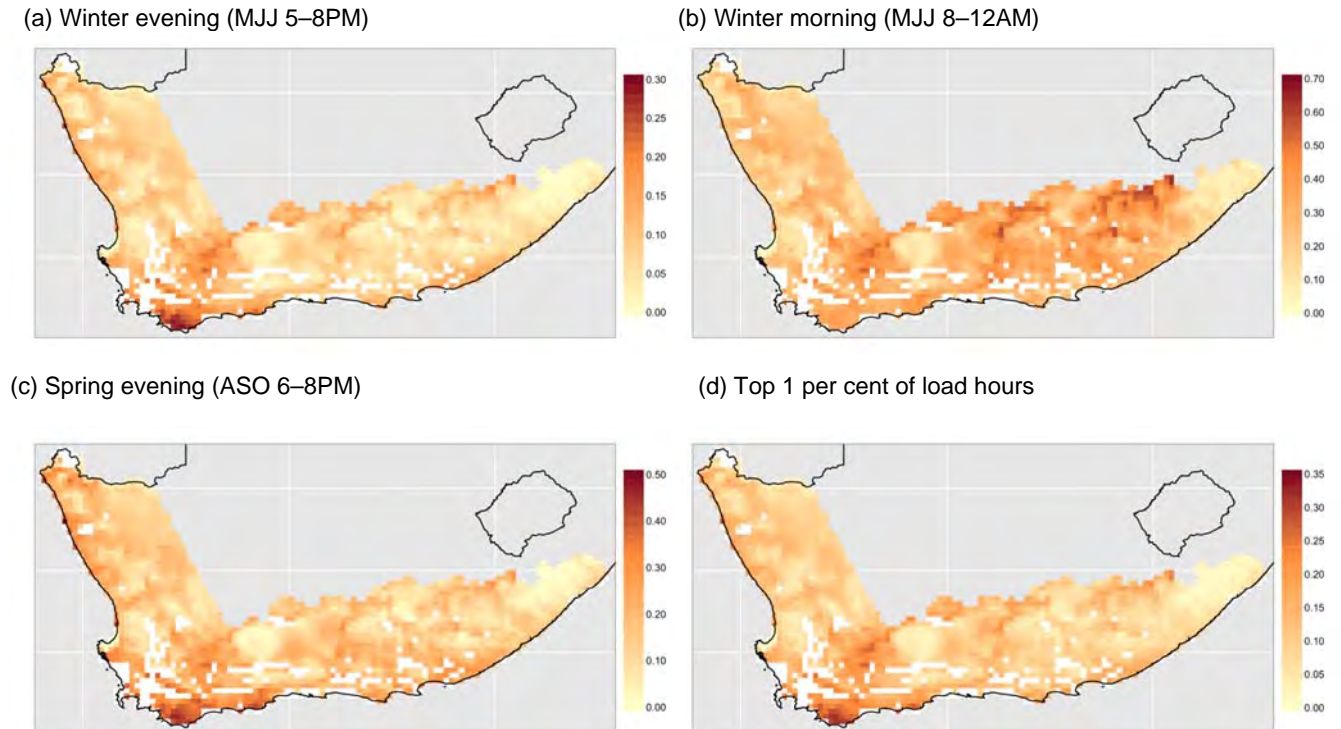
Long-term CSP (6-hour storage) generating efficiency is up to 50 per cent among the highest-efficiency sites in the Northern Cape (Figure 4). Notice that the best CSP sites show a different geographic distribution than for PV, reflecting the different solar irradiance and temperature dependence of the technologies. Similar to PV, there are some moderately good CSP resources located closer to population centres in the Western Cape and Pretoria/Johannesburg area.

4.3 Peak period efficiency across space

The performance of WSP technologies during periods of high electricity demand is of particular interest from the standpoint of integration and reliability. Section 5 describes the generation of projected hourly electricity demand for the South Africa power system in 2040. On the basis of those results, three periods of particularly high electricity demand are identified: (1) winter evenings (MJJ [May, June, July] 5–8PM); 2) winter mornings (MJJ 8–12AM); and (3) spring evenings (ASO [Aug., Sept., Oct.] 6–8PM). A fourth 'period' is also included, consisting of hours exhibiting load

within the top 1 per cent of all hours, given that information derived from this hourly subset is known to be useful for approximating the ability of WSP resources to contribute to reliability targets (Milligan and Porter 2008). Mean generating efficiency maps were created for each of the periods, using the same spatial interpolation technique described above for long-term mean efficiency.

Figure 5: Mean modelled wind farm generating efficiency, by high-load period (1996–2005)



Source: Authors' creation (data modelled by SAM).

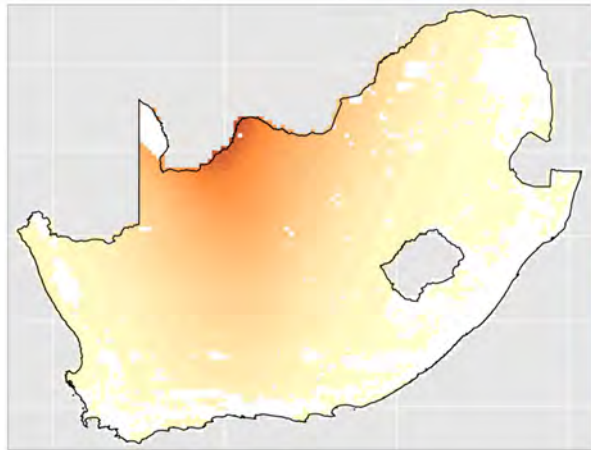
Among the four periods in Figure 5, wind generating efficiency is highest during winter mornings, with the best locales reaching mean hourly capacity factors of 70 per cent. Conversely, during winter evenings (the primary peak period), the best sites reach (on average) only 30 per cent. The geographic location of the best sites is also very different between periods. During winter mornings, the best locales are found in the north-east reaches of the Eastern Cape. In the evenings, however, the best locales congregate in the Western Cape, south-west of Cape Town. This is consistent with diurnal wind speed patterns that favour daytime wind power production over evenings (see Figure 8).

PV and CSP generating efficiency during peak periods generally reflects east-to-west variations in the height of the sun but with technology-specific differences (Figures 6 and 7). In the case of PV, efficiency is highest during winter mornings, with the evening peak periods exhibiting considerably lower output. Note, however, that the locales most suitable for winter morning generation are to the east and do *not* overlap with those identified in Figure 3 as most suitable for long-term efficiency.

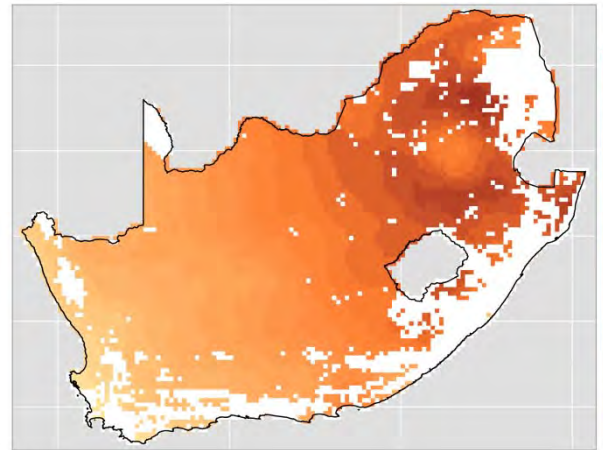
Due to thermal inertia and storage, winter mornings are the period of *lowest* generating efficiency in the case of CSP. The other periods (dominated by evening hours) exhibit much higher efficiencies in the best locales but with geographic differences between periods. In particular, the sites most suitable for spring evening generation are quite different from those most suitable for winter evenings—and both are different from the best long-term locales identified in Figure 4.

Figure 6: Mean modelled utility-scale PV generating efficiency, by high-load period (1996–2005)

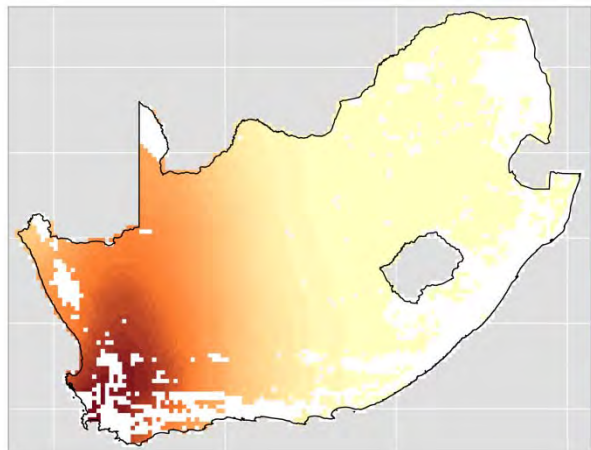
(a) Winter evening (MJJ 5–8PM)



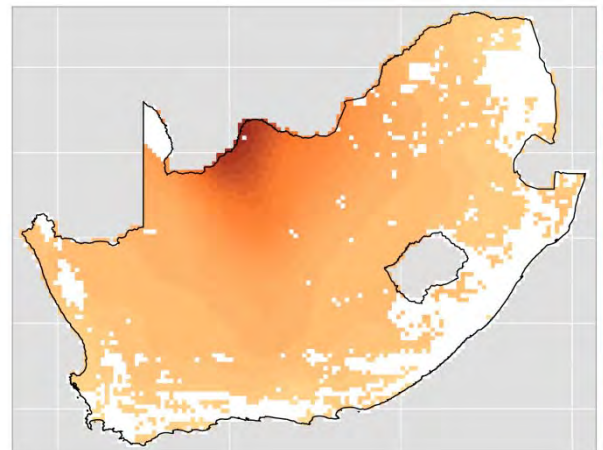
(b) Winter morning (MJJ 8–12AM)



(c) Spring evening (ASO 6–8PM)



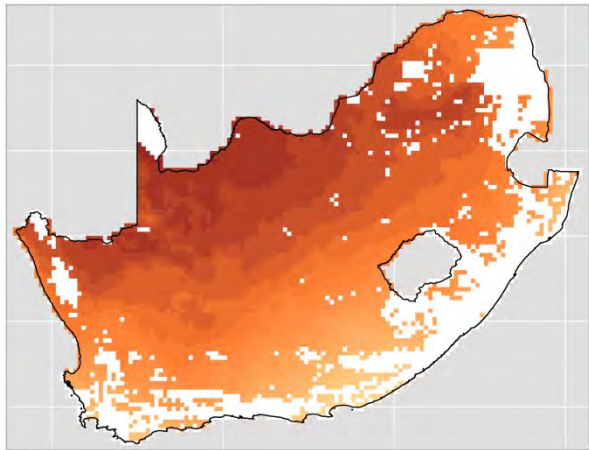
(d) Top 1 per cent of load hours



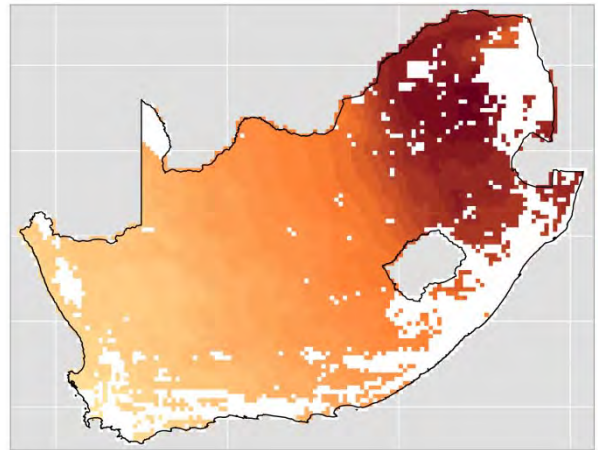
Source: Authors' creation (data modelled by SAM).

Figure 7: Mean modelled CSP generating efficiency, by high-load period (1996–2005)

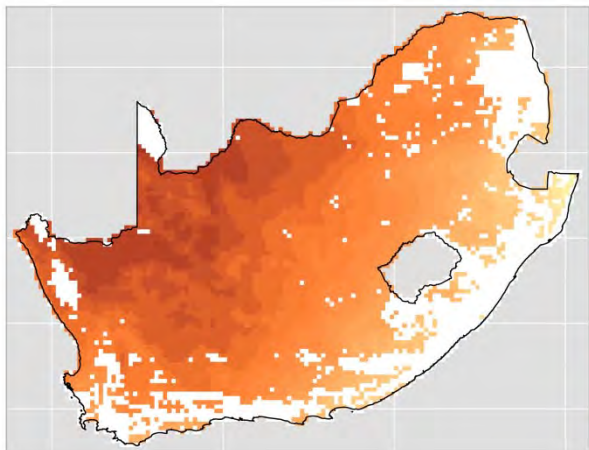
(a) Winter evening (MJJ 5–8PM)



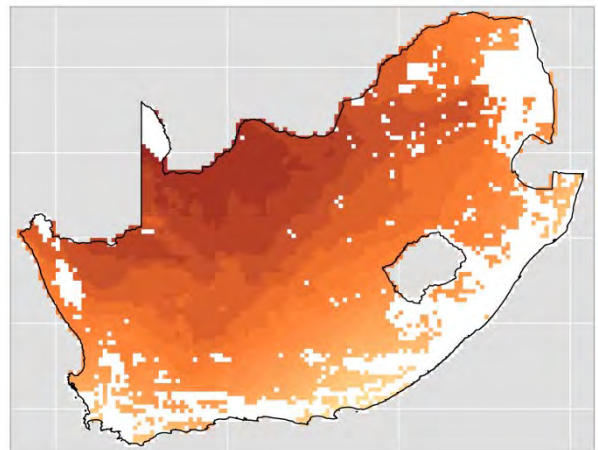
(b) Winter morning (MJJ 8–12AM)



(c) Spring evening (ASO 6–8PM)



(d) Top 1 per cent of load hours

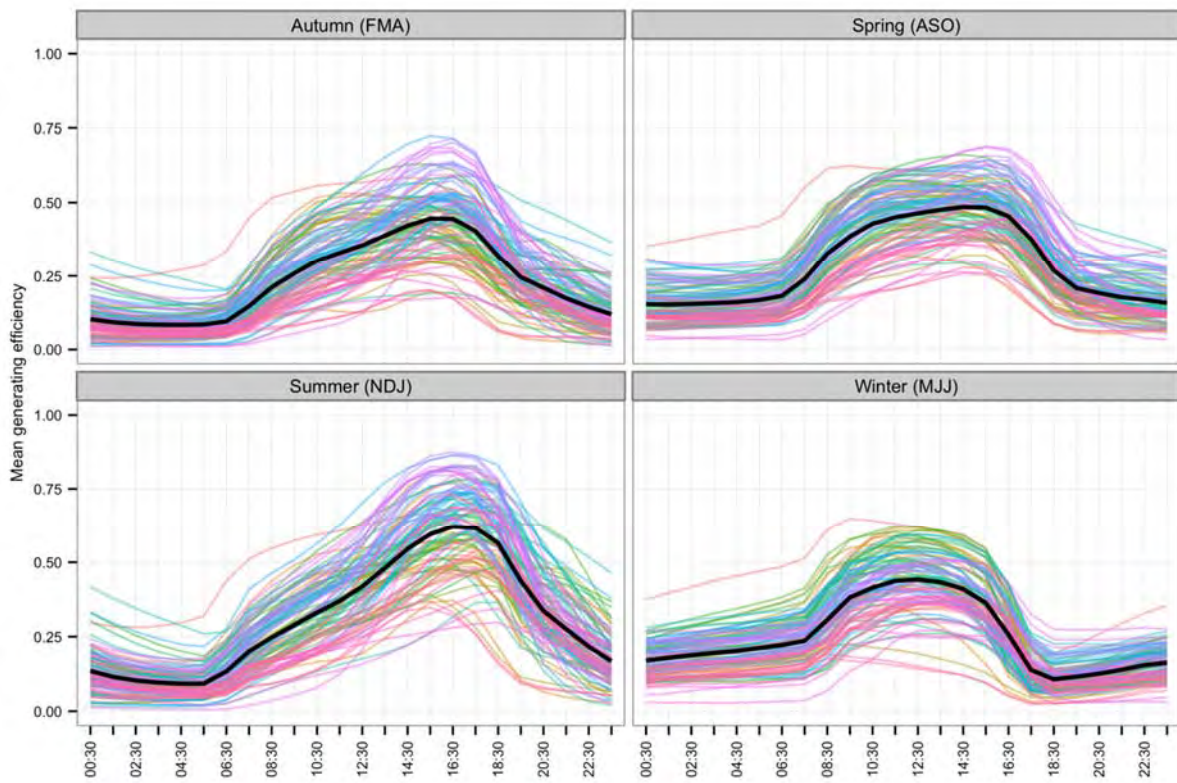


Source: Authors' creation (data modelled by SAM).

4.4 Diurnal trends across seasons

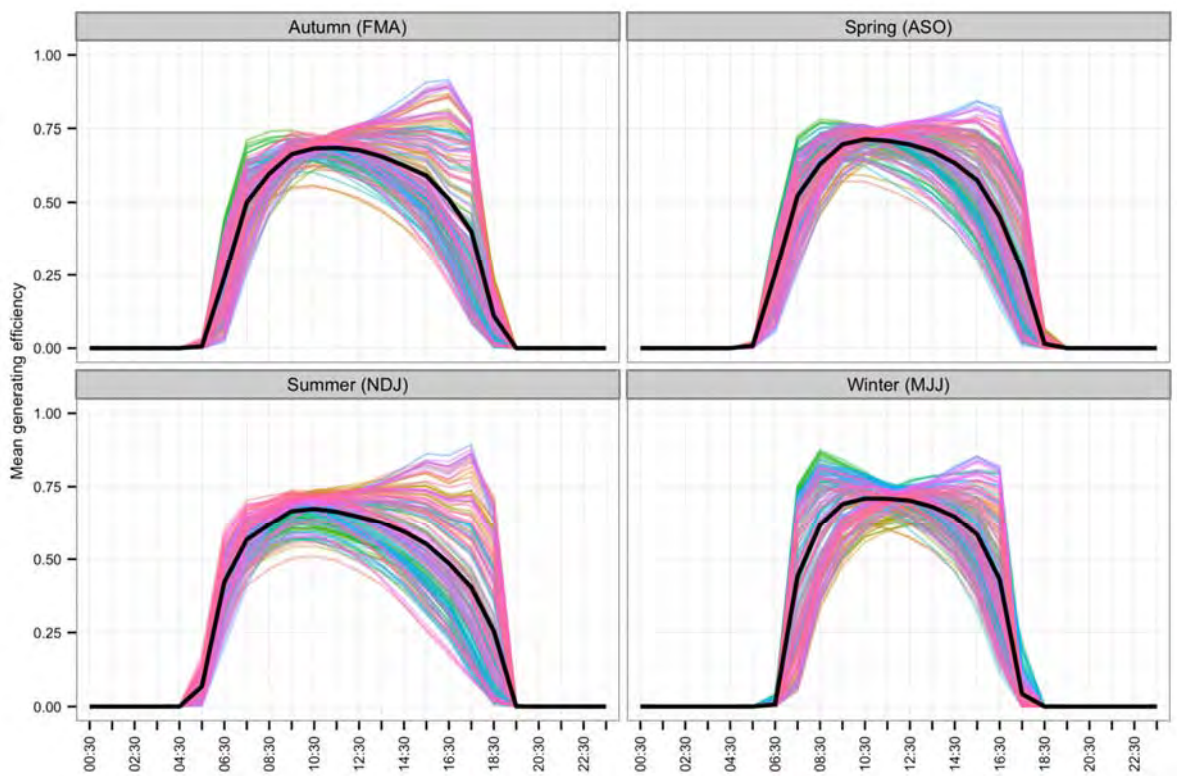
The generating efficiency of WSP technologies often varies predictably over the course of a day (diurnal pattern) and seasons. The diurnal behaviour of WSP determines the nature of its interaction with load and conventional technologies within the power system. Figures 8 through 10 summarize a large amount of hourly data to reveal typical diurnal patterns, by season and WSP technology, across the whole of South Africa. Each coloured line shows the mean diurnal pattern for an individual modelled site. The black line shows the mean diurnal pattern across all modelled sites. Although certain trends are evident, there is also considerable variability as a result of the inherent spatial diversity.

Figure 8: Mean diurnal generating efficiency, by season, for 110 modelled wind sites (1996–2005)



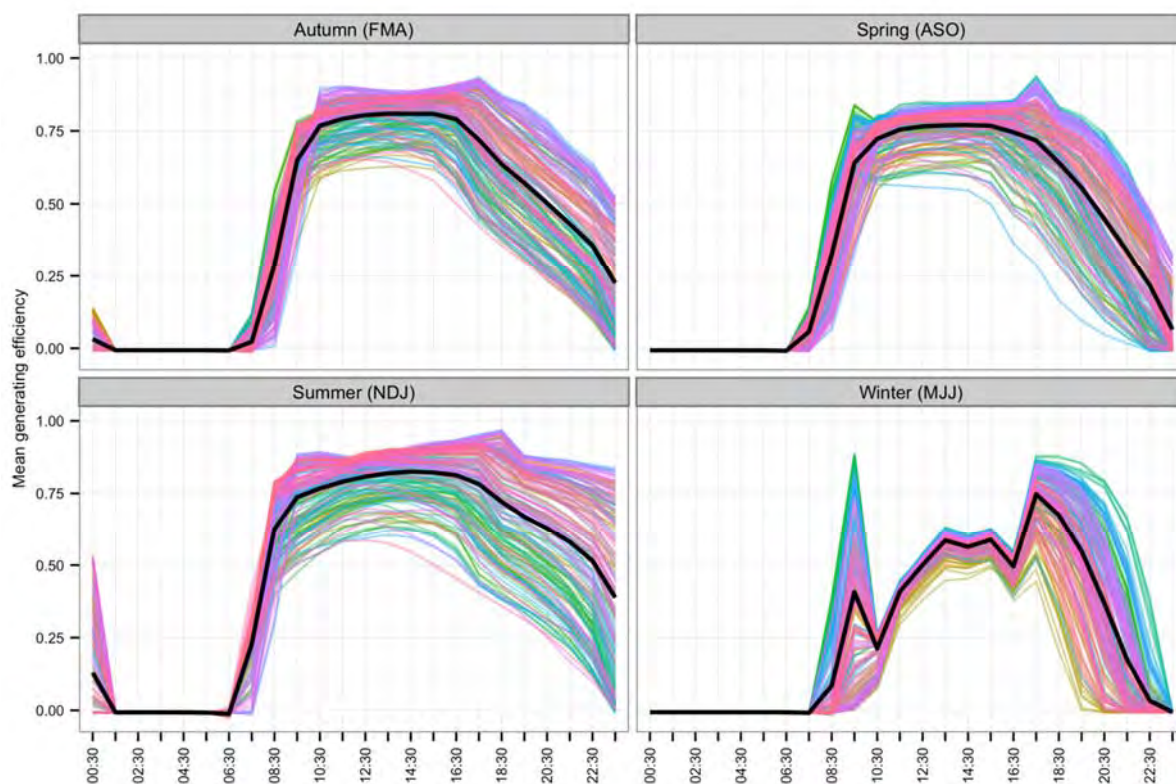
Note: FMA – Feb., March, April; NDJ – Nov., Dec., Jan.
Source: Authors' creation (data modelled by SAM).

Figure 9: Mean diurnal generating efficiency, by season, for 176 modelled PV sites (1996–2005)



Source: Authors' creation (data modelled by SAM).

Figure 10: Mean diurnal generating efficiency, by season, for 178 modelled CSP sites (1996–2005)



Source: Authors' creation (data modelled by SAM).

Wind power resources within the assessed region show a clear tendency towards higher generating efficiency during the day. The general diurnal pattern of higher daytime efficiency is evident across all four seasons. The summer (NDJ) diurnal pattern is particularly pronounced, with efficiency peaking in the late afternoon. Winter (MJJ) generating efficiencies are significantly lower, with a less pronounced daytime peak and particularly low early evening output.

PV power resources exhibit a predictable diurnal pattern, though with significant variation reflecting geographic and seasonal differences. On average, summer generating efficiency remains relatively high into early evening, with some locales showing mean capacity factors in excess of 50 per cent in the 6–7PM period. Winter generation truncates earlier in the day. The peak efficiency over the course of a given day does not differ much between seasons.

CSP resources are able to extend generation far into the evening, particularly in summer where some locales exhibit capacity factors in excess of 50 per cent through midnight. The clearly different winter diurnal profile reflects the modified plant control algorithm used during that season (see Section 3). The algorithm effectively suppresses electricity generation during midday and early afternoon hours in order to charge the storage system and maximize output during peak period winter evenings. Notice the considerable variation across sites in CSP generating efficiency during evening and night-time hours. Because performance during those hours is largely determined by the accumulation of solar energy over the course of the day, relatively small daytime differences in generating efficiency are not inconsistent with large differences in generating efficiency after sunset.

5 Hourly electricity demand

Data on hourly, system-wide electricity demand (load) in South Africa during 2010 and 2011 were provided by Eskom staff. The power sector scenarios described in Section 6 are for the year 2040, requiring present-day load be projected to that date.

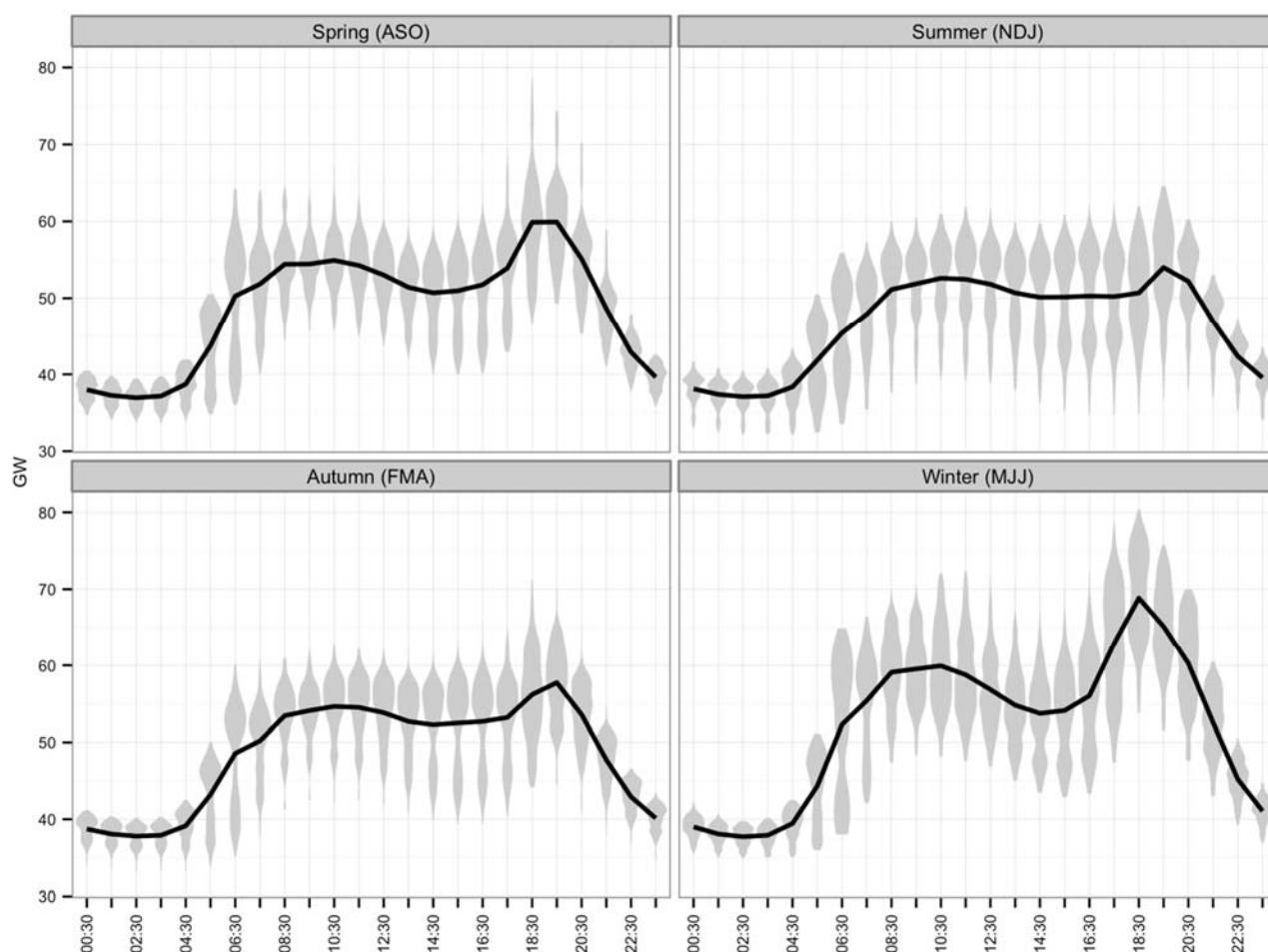
Between the present and 2040, electricity demand in South Africa is expected to increase appreciably. The IRP provides projected mean and maximum load for South Africa through 2030, which are then linearly extrapolated to 2040. Mean hourly load is assumed to grow 75 per cent (from 28 GW to 49 GW); maximum annual (peak) load is assumed to grow nearly 120 per cent (from ~37 GW to 80 GW). These figures account for assumed demand side management efforts through 2030, per the IRP. In addition, it is assumed that minimum annual load is 40 per cent of peak load in 2040, based on load behaviour in New South Wales, Australia, which is thought to provide a developed-country comparator in a similar climate.

Using the assumed changes to minimum, mean, and maximum load, the 2010–11 time series is scaled to 2040. The differing rates of change in mean and maximum load imply that higher-load hours will grow disproportionately faster than lower-load hours, but the exact nature of the changes to the load profile is unclear. In the absence of such information, the scaling process is necessarily arbitrary.

The technique used here assumes that higher-load hours increase exponentially faster than lower-load hours. Let r be a vector containing the ratio of hourly load to the minimum annual load over 2010–11. Let R be an analogous vector of ratios used to scale load in 2011–12 to 2040. Based on the assumed changes described above, R must range from 1 to 2.5 with a mean value of 1.53. I assume that $R = S(rx)$, where $x > 1$ and S is a function that linearly scales rx between 1 and 2.5. The value of x is determined numerically such that the mean of R is 1.53, which occurs at $x = 2.18$.

Figure 11 shows the resulting distribution of load, by season and time of day, for 2040. The solid black line shows mean load; the grey violin plots show the relative probability distribution across two years of hourly data. The highest-load hours most often occur during winter evenings (MJJ) between 5PM and 8PM. There are two additional periods of relatively high load: winter mornings (MJJ 8AM to noon) and spring evenings (ASO 6PM to 8PM).

Figure 11: Assumed 2040 system-wide load profile and distribution, by season



Source: Authors' creation (based on data provided by Eskom).

6 Power system scenarios and modelling

Sections 6 and 7 use the data developed above to simulate the economic and environmental performance of three different WSP deployment patterns in the year 2040. An Eskom planning scenario is used as the basis for this exercise.

This section describes the 'default' Eskom scenario and the WSP spatial deployment pattern it implies. Then, a simple power system model is introduced that simulates hourly system performance with respect to reliability, carbon dioxide (CO₂) emissions, and overall cost, taking into account the spatiotemporal variability inherent to WSP resources. Finally, two variations on the original scenario are developed (Variation A and Variation B) by optimizing the location and quantity of WSP technologies to minimize the cost of CO₂ abatement. Simulation results for all three scenarios are presented in Section 7.

6.1 Default Green scenario

Eskom has created a number of power system planning scenarios for WSP expansion through the year 2040, guided by the IRP (Eskom 2012). One of those scenarios, called the 'Green' scenario, envisions total WSP capacity in excess of 46.5 GW in 2040.

The Eskom Green scenario is particularly aggressive with respect to WSP deployment, which makes it especially interesting from the standpoint of integration and reliability. The approved IRP currently envisions 18.8 GW of WSP by 2030. The Green scenario increases that figure appreciably by 2040, largely due to the exclusion of new nuclear capacity. In contrast, the IRP relies on the addition of 9.6 GW of nuclear capacity by 2030 to meet electricity demand and emissions targets. Table 1 gives the installed capacity and level of penetration, in 2040, for each generating technology in the default Green scenario.

Table 1: Installed capacity by 2040 in default Green scenario

Generating technology	MW installed by 2040	Penetration (% of total)
Coal	41,071	36.4
Open-cycle gas turbine (OCGT)	7,780	6.9
Combined-cycle gas turbine (CCGT)	7,170	6.3
Pumped storage (hydro)	2,912	2.6
Nuclear	1,800	1.6
Imports (hydro)	4,759	4.2
Biomass	890	0.8
Wind	23,000	20.4
PV	12,600	11.1
CSP	10,960	9.7
Total	112,942	100%

Source: Authors' creation (based on data from the IRP [Eskom 2012]).

Given the high penetration of WSP in the Green scenario, the performance of the power system is strongly affected by the assumed location of WSP facilities. Eskom has identified geographic areas (zones) where it deems future deployment of different WSP technologies to be likely. The Green scenario specifies how much wind and CSP capacity to allocate to each of the relevant zones is needed. Geographic zones are also identified for PV deployment, but no quantities are assigned to specific zones. Consequently, I assume that the PV fleet is distributed evenly across the identified zones.

The technology zones identified by Eskom are relatively large. Within a given zone, I assume that projects are ultimately sited in locales (grid cells) with the highest long-term capacity factors. This is a reasonable assumption given the desire of project developers to maximize long-term electricity output. Figure 12 (following section) displays the resulting WSP spatial deployment pattern implied by Eskom's Green scenario for 2040, given the aforementioned assumptions.

6.2 Simple power system model

Given assumed quantities of conventional generation and a pattern of spatial deployment for WSP technologies, it is possible to simulate system performance in terms of CO₂ emissions, reliability, and cost. To do this, a simple, single-node power system model is created. It assumes there are no transmission or distribution constraints or costs.

Given a particular WSP deployment pattern, the model uses data described in Section 4 to calculate the aggregate (i.e. fleet-wide) hourly WSP power generation for a 10-year period. In conjunction with the load time series described in Section 5 and the conventional generation quantities in Table 1, the loss of load probability (LOLP) is calculated for each hour. The LOLP gives the likelihood that electricity supply will be insufficient to meet demand, taking into account the probability of unexpected outages among conventional generators.⁶ Summing the LOLP over 10 years of hourly data gives the loss of load expectation (LOLE), usually expressed as hours per year, which is a standard measure of system reliability. Although alternative reliability metrics are possible (e.g. unserved energy), LOLE is convenient and easily benchmarked.⁷

After making an initial LOLE calculation, the model then determines how to adjust the Green scenario's OCGT capacity to achieve the specified LOLE. A LOLE target value of 0.1 days per year is used, as this is commonly cited as a typical level of planning reliability in developed-country power systems (NERC 2012). To achieve the target LOLE, the model may add or subtract OCGT capacity from the Green scenario initial capacity of 7.78 GW.

The model assumes that pumped storage and imported hydroelectric capacity is available when it is likely to be needed most. This is accomplished by allocating pumped storage and imported hydroelectricity generation to hours where the net load (load minus WSP output) is highest, subject to the constraint that the long-term (net) capacity factors for pumped storage and hydroelectric imports must be 0.2 and 0.4, respectively, as specified in the IRP.

The model also imposes a 'turndown rate' on coal and nuclear generators, reflecting the need to maintain a minimum level of thermal output and preventing them from dropping below an hourly capacity factor of 0.35 (Ihle and Owens 2004). If WSP, pumped storage, and hydroelectric imports are so large in a given hour that coal and nuclear generators would be forced below the turndown rate, the former are curtailed accordingly.⁸

The 10-year, hourly economic and environmental performance of the system is calculated, assuming that generating technologies are prioritized by their marginal running cost—that is, within a given hour, the system utilizes WSP generation first and only resorts to relatively expensive gas generation when absolutely necessary to meet demand. Hourly operating costs, annualized capital costs, and hourly CO₂ emissions are also calculated, using technology and fuel cost assumptions and CO₂ emissions factors taken from the IRP.

Finally, the average cost of CO₂ abatement is estimated. Abatement cost calculations require a baseline or counter-factual scenario without WSP. Consequently, the model is first optimized to determine the minimum annual cost of meeting electricity demand in the absence of WSP—that is, a low-cost, high-pollution scenario. The optimization uses the Green scenario's default installed capacity values (Table 1), but replaces WSP with the least-cost combination of coal, OCGT, and

⁶ The LOLP calculation treats WSP generation as a negative load, following the convention outlined by Keane et al. (2011). The cumulative outage probability table (COPT) for conventional generators is constructed using the recursive convolution algorithm described in Makarov et al. (2010).

⁷ The concept of power system 'reliability' has a number of components (e.g. frequency regulation), but the focus here is on what is usually (and more accurately) referred to as 'system adequacy'. I use 'reliability' throughout given its greater familiarity with a general audience, but its use is meant to be synonymous with 'adequacy'.

⁸ Coal and nuclear plant thermal efficiency is assumed constant. In practice, efficiency declines at lower capacity factors. The inclusion of ramp rate constraints was considered, but the typical, hour-to-hour variability observed within the WSP fleet was such that the constraint was deemed minimal and consequently excluded. Ramp rates are likely to be important if higher-resolution WSP resource data are used and/or spatial transmission constraints are imposed.

CCGT. The overall cost and CO₂ emissions resulting from this least-cost system are used as the comparator when calculating the cost of CO₂ abatement associated with the introduction of WSP.

6.3 Variations on the Green scenario

In addition to the default Green scenario described above, two variations are constructed. The first, called Variation A, is identical to the Green scenario, except that the *location* of WSP capacity in 2040 is optimized to find the spatial arrangement that minimizes the cost of CO₂ abatement. The second, called Variation B, *also* allows the *quantity* of WSP capacity to be optimized, subject to the constraint that a total of 46.5 GW of WSP capacity be installed in 2040.

The task of optimizing the location of WSP resources presents a non-trivial optimization problem. The number of potential combinations of quantities, technologies, and locations is immense. Traditionally, power system planning models have relied on linear programming (LP) techniques (e.g. Short et al. 2011). While efficient and robust, LP models require problems to be specified in a particular form, preventing, for example, direct computation of LOLP/LOLE reliability metrics using long-term hourly time series.

The alternative approach used here employs an evolutionary search or ‘genetic’ algorithm (GA) to ‘evolve’ an initial solution set (or ‘population’) towards the global minimum, using rules for gene mutation and crossover borrowed from evolutionary biology. Specifically, I use the GENOUD algorithm as implemented in the ‘Rgenoud’ package for the R programming language (Mebane and Sekhon 2011). This technique allows the objective function and parameter constraints to be specified in any manner. While GAs are not definite, they are quite effective at identifying the global optimum, provided the initial population is sufficiently large (Lobo and Lima 2007).

The parameters to be optimized include the quantity of WSP capacity to be deployed in a given grid cell for a given technology. Section 4 presents spatiotemporal generating efficiency data for a relatively large number of modelled WSP sites and interpolates that data across all grid cells in the study area via universal kriging. It is possible to condense this data without losing information, in an effort to reduce the number of parameters needed to obtain an optimized deployment pattern.

The SKATER clustering algorithm is again used to cluster modelled WSP sites, grouping those with similar diurnal generating efficiency patterns across seasons. Within each cluster, all feasible grid cells are ranked from highest long-term capacity factor to lowest. It is assumed that, within a given cluster, the sites with the highest long-term capacity factors are given preference.

For each cluster, a function is constructed that describes how a given quantity of capacity is to be allocated across individual grid cells. These functions are used within the model objective function to quickly compute the 10-year, hourly electricity output time series for a given capacity in a given cluster. This clustering approach is used to reduce the number of model parameters to a more manageable number for the purposes of optimization, while retaining much of the spatiotemporal information in the underlying time series database.

The simple power system model is optimized using the GENOUD algorithm to identify particular patterns of WSP deployment that minimize the cost of CO₂ abatement. Variation A results from optimizing *only the location* of WSP facilities; the total installed capacity of each WSP technology is the same as in the default Green scenario (Table 1). Variation B results from optimizing *both the*

location and quantity of individual WSP technologies, subject to the constraint that a total of 46.5 GW of WSP capacity be installed.⁹

One could alternatively minimize (or maximize) an economic or environmental metric other than the cost of CO₂ abatement; for example, minimizing total emissions or cost. However, the abatement cost captures the inherent trade-off between economic and environmental objectives, thereby providing a more comprehensive metric for ranking deployment options. As shown in the following section, optimizing with respect to abatement cost allows for the identification of deployment strategies that are not cost- or emissions-minimizing but likely to be preferable from a policy perspective.

7 Simulation results

Table 2 summarizes simulation results for the default Green scenario as well as Variation A and Variation B. The Green scenario exhibits an average cost of CO₂ abatement in 2040 of US\$26.5 per tCO₂ (total carbon dioxide; 2010 dollars). Variation A and variation B, which optimize the location and quantity of WSP technologies so as to minimize abatement costs, result in commensurate values of US\$22.8 and US\$15.7 respectively.

Table 2 also identifies other differences between scenarios. Note that the default Green scenario and Variation A, by design, contain the same installed capacity for wind, PV, and CSP. Yet, the average capacity factor across these technologies differs considerably between scenarios, with Variation A siting facilities such that the WSP fleet generates about 6 per cent more electricity than in the Green scenario.

Variation B results in a very different balance of WSP technologies. The abatement cost-minimizing solution returned by the GA contains nearly 39 GW of PV capacity, compared to just 2.8 GW of wind and 4.9 GW of CSP capacity. This dramatic shift towards PV drives down the annualized cost of operating the power system (due to the projected low capital cost of PV in 2040) but results in slightly higher CO₂ emissions. However, since the cost savings are relatively greater than the emissions increase, the cost of CO₂ abatement declines.

As noted in Section 6, the model internally adjusts the amount of OCGT capacity to ensure a long-term LOLE value of 0.1 days per year, based on 10 years of hourly simulation and the particular WSP deployment pattern. The dramatic shift to PV in Variation B is only possible because of significant changes to the quantity of gas generating capacity. Section 4 shows that PV has little ability to contribute electricity during high-load evening periods. Variation B responds by building out OCGT capacity, as evidenced by an increase in the reserve margin. With respect to the cost of CO₂ abatement, the economic and environmental cost imposed by the building and using of gas capacity, given the IRP's assumptions, do not outweigh the benefits of increased PV capacity.

Figures 12, 13, and 14 display the WSP spatial deployment patterns returned for the default Green scenario, Variation A, and Variation B, respectively. These are the deployment patterns underlying the results in Table 2.

⁹ The Variation A and Variation B models contain ~90 parameters (clusters) each. Lobo and Lima (2007) cite analysis by Pelikan et al. (2003) that asserts GA population size should be between approximately $p^{1.05}$ and $p^{2.1}$, where p is the number of parameters. With this in mind, a population size of 8,000 was selected and the two optimizations run simultaneously, each using a single compute core. Each run required ~700,000 objective function evaluations to settle on a solution, requiring ~78 core-hours on a 2.5 GHz Intel Core i5 processor.

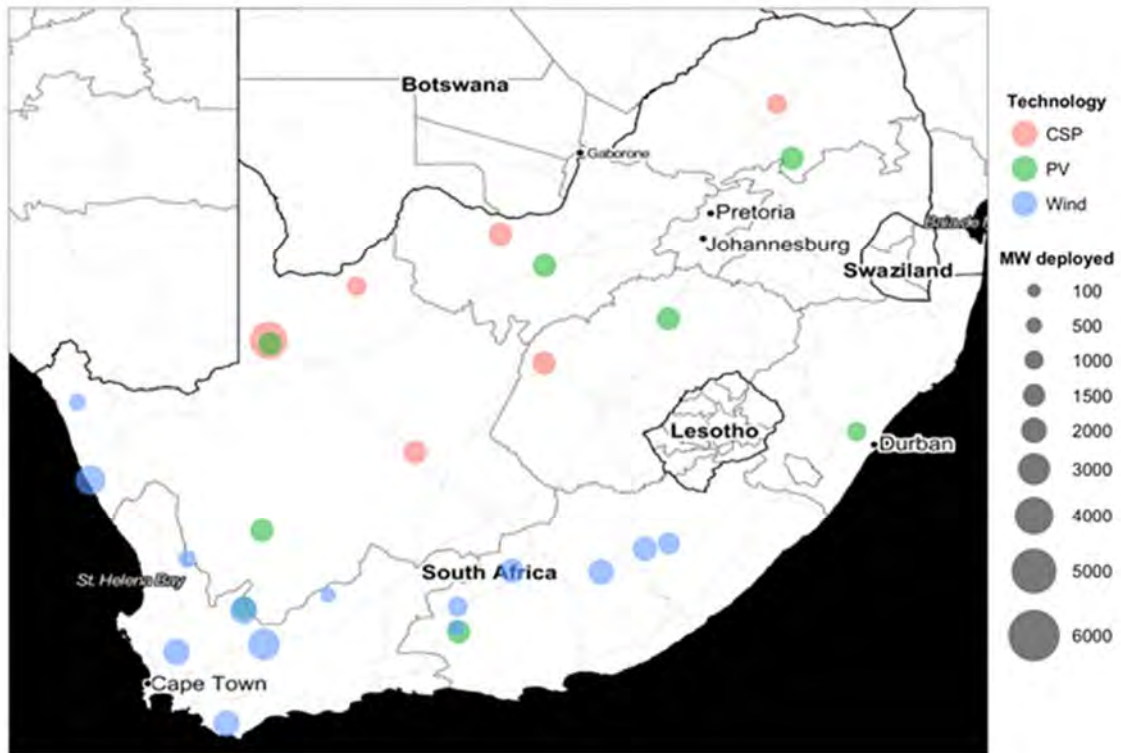
The default Green scenario deployment pattern (Figure 12) exhibits relatively wide-ranging solar power dispersion, reflecting Eskom’s assumptions regarding areas likely to see WSP development. By comparison, Variation A and Variation B consolidate PV and CSP capacity in the Northern Cape, utilizing the highest-efficiency locales. Variation B (which is dominated by PV) disperses PV capacity throughout the Northern Cape and, to a much smaller degree, the Western Cape and North West Province. Variation A is not significantly different than the default Green scenario is in terms of wind power siting, though the former does shift capacity away from the coastal Northern Cape and into the Western and Eastern Cape where the wind resource is deemed more desirable.

Table 2: Summary of simulation results

	Green scenario	Variation A	Variation B
Average abatement cost in 2040 (2010 US\$ per tCO2)	US\$26.5	US\$22.8	US\$15.7
Average annual emissions in 2040 (MtCO2)	236	229	241
Average annualized system cost in 2040 (2010 billion US\$)	26.3	26.1	25.1
Average annual WSP electricity delivered in 2040 (TWh)	138.8	147.1	132.2
Reserve margin (%)	38.5	36.9	44.2
Onshore wind average capacity factor (%)	32.6	33.5	35.9
PV average capacity factor (%)	29.0	32.0	30.0
CSP (6hr) average capacity factor (%)	42.9	46.2	46.2
Onshore wind capacity in 2040 (GW)	23.0	23.0	2.8
PV capacity in 2040 (GW)	12.6	12.6	38.8
CSP (6hr) capacity in 2040 (GW)	11.0	11.0	4.9

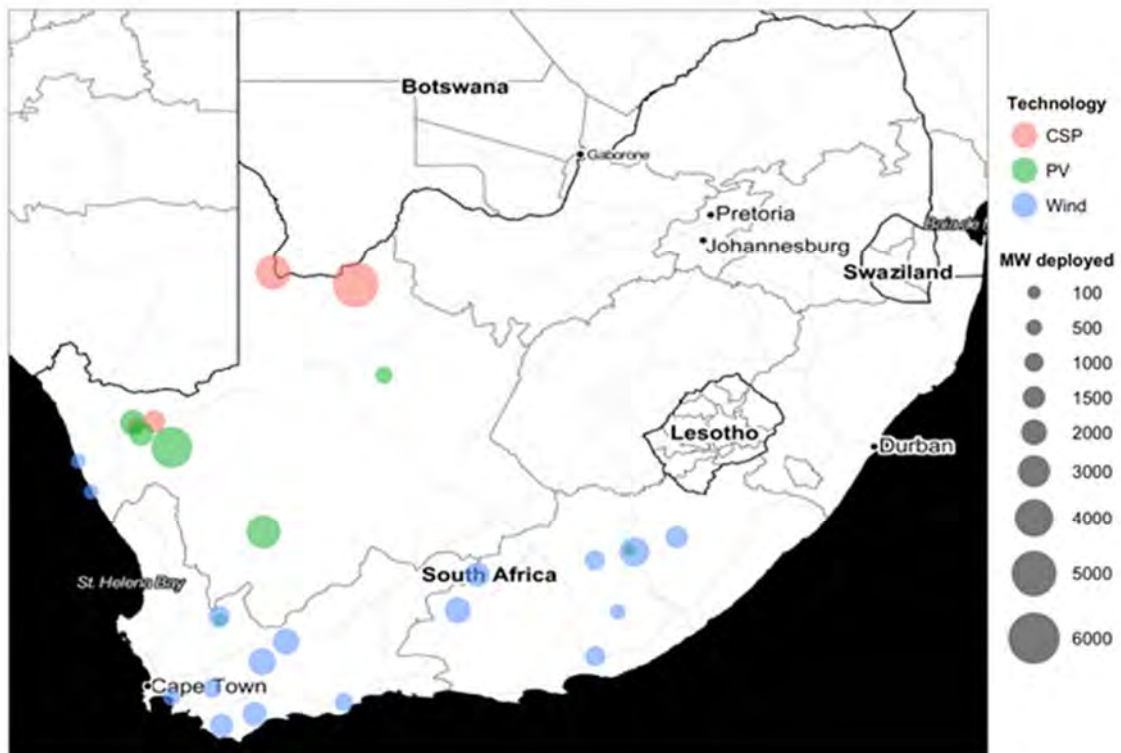
Source: Authors’ creation.

Figure 12: Assumed WSP spatial deployment pattern in 2040 for default Green scenario



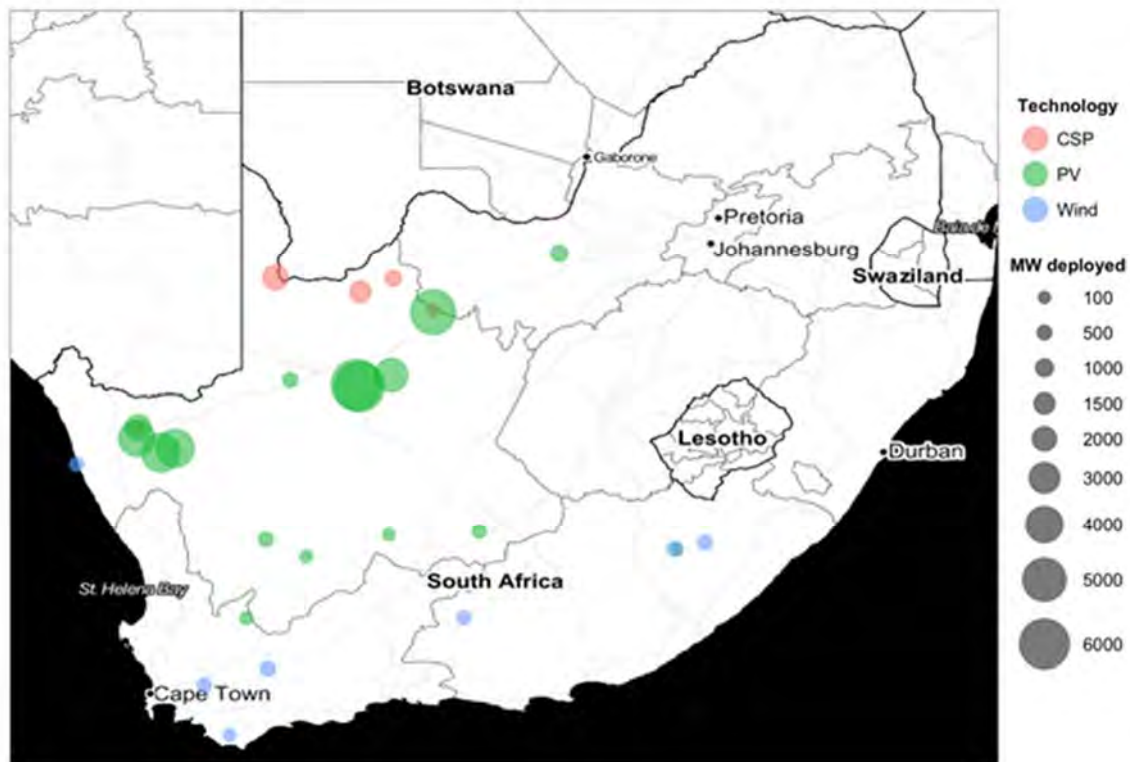
Source: Authors' creation.

Figure 13: WSP spatial deployment pattern in 2040 for Variation A scenario



Source: Authors' creation.

Figure 14: WSP spatial deployment pattern in 2040 for Variation B scenario



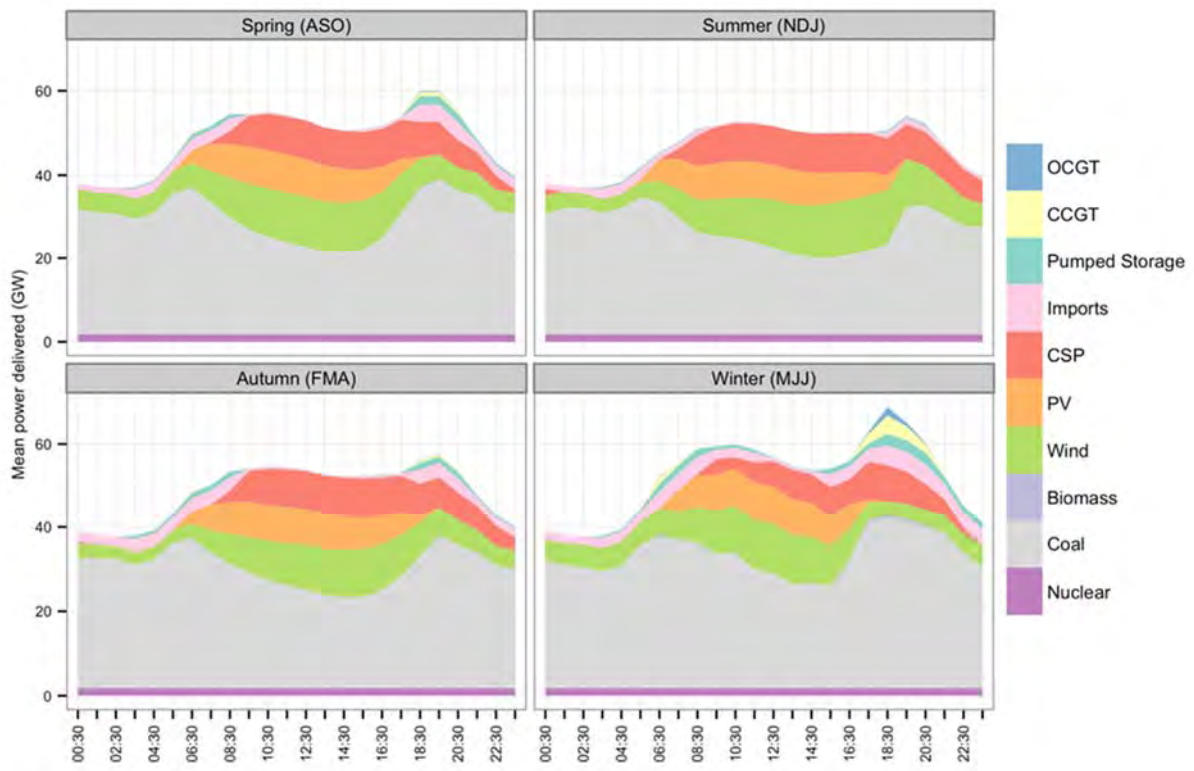
Source: Authors' creation.

Figures 15, 16, and 17 show the mean diurnal generation profile, by season, for the default Green scenario, Variation A, and Variation B, respectively. Each figure shows how, on average, the various technologies in the power system combine to meet the system-wide load. The data underlying these figures include 10 years of hourly simulation results. In all cases, the winter evening peak period exhibits increased use of OCGT and CCGT generators to meet the increased demand.

It is difficult for the eye to discern differences between the mean diurnal generation profiles for the default Green scenario and Variation A. Both exhibit broadly similar patterns in the magnitude and timing of power generation among different technologies. However, even the relatively small differences resulting from improved WSP siting lead to significant differences in the average cost of CO₂ abatement (Variation A being 14 per cent lower, as noted in Table 2).

Variation B (Figure 17), on the other hand, is clearly different. The large quantity of PV capacity results in a dramatic daytime decline in coal power output (replaced by PV power). Coal power then ramps up quickly to help address higher-load evening periods in which the contribution from WSP is quite small. Figure 17 also clearly shows the increased prominence of gas generation in meeting high-load periods, as evidence by the higher reserve margin noted in Table 2.

Figure 15: Mean diurnal generation profile in 2040 for default Green scenario, by season



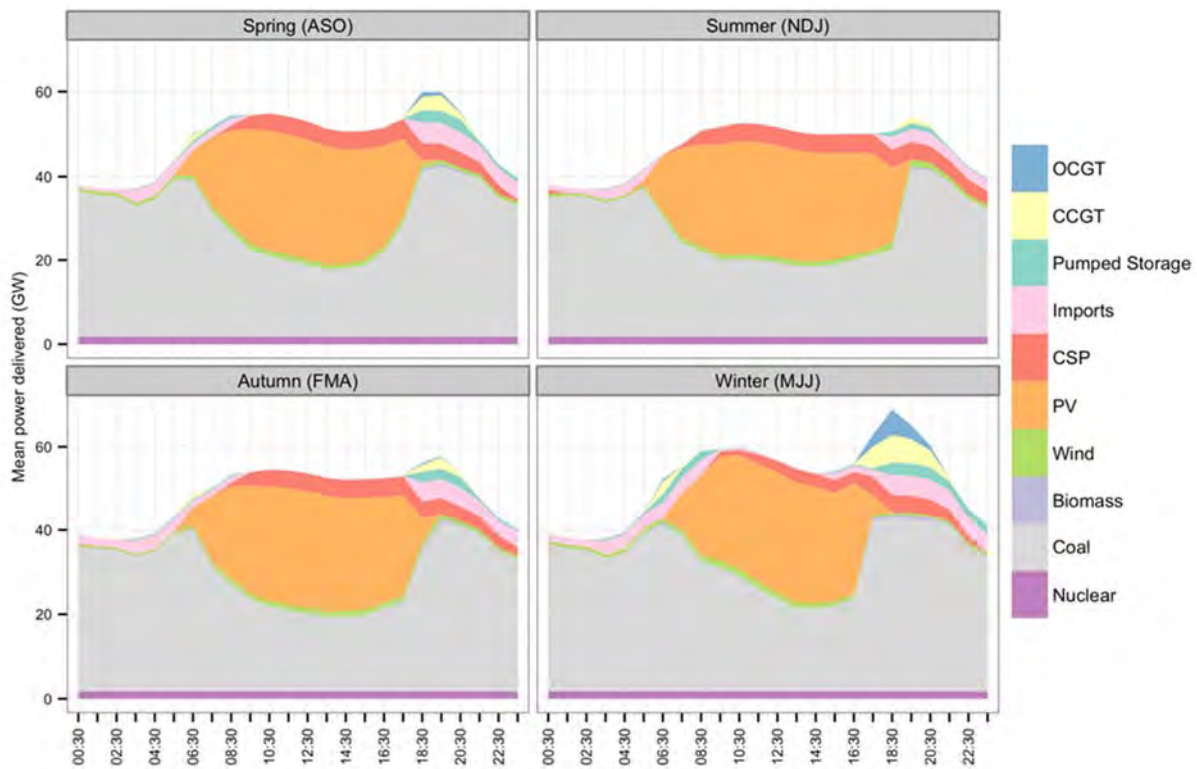
Source: Authors' creation.

Figure 16: Mean diurnal generation profile in 2040 for Variation A scenario by season



Source: Authors' creation.

Figure 17: Mean diurnal generation profile in 2040 for Variation B scenario, by season



Source: Authors' creation.

8 Discussion

As noted in Section 1, an important objective of this research is to demonstrate the potential for new data and modelling techniques to capture important spatiotemporal dynamics in power systems with high penetration of WSP. The results presented in Section 7 suggest that the use of such techniques to explicitly optimize the location and quantity of WSP technologies could potentially identify deployment strategies that significantly reduce the cost of CO₂ abatement, while ensuring reliability.

The model presented here is an admittedly simplistic representation of South Africa's power system. Most notably, it ignores transmission issues that could play an important role in guiding cost-effective deployment of WSP. And since the model is a simple, single-node model, load variation and balancing across space are effectively ignored.

However, one of the advantages of the technique introduced here is its flexibility. The GA optimization approach allows for model specification to take on any form (even sub-optimization routines), and the WSP spatial clustering process provides a defensible way to scale the problem size for available computing resources. Moreover, GA optimization is typically 'embarrassingly parallel', offering the option to utilize cloud computing for very large simulations.

A primary task for future research is to incorporate transmission costs and constraints into the modelling framework. This will require data and institutional support from South Africa's grid operator, and the creation of transmission infrastructure cost assumptions, as the IRP does not currently address this subject. It is not clear if inclusion of transmission costs and constraints would

necessarily alter the optimal mix or location of technologies, but it would increase the cost of CO₂ abatement.

Further work is also needed to simulate system expansion over time (e.g. 2015 through 2040 with WSP deployment or emissions targets for each year) and uncertainty in critical cost assumptions (e.g. Monte Carlo analysis over a range of future technology and fuel costs). None of these advances pose overwhelming technical challenges—they can be introduced to the existing model given its flexibility—but they will require buy-in by stakeholders in South Africa’s power sector. In short, the barriers are likely more political than technical.

The need to embed future planning models (whether this one or others) in a probabilistic framework is made clear by the dramatic shift towards PV in Variation B. This result is driven, in large part, by the IRP’s assumption of declining PV capital costs over time. But the pace and magnitude of cost reductions is, in fact, uncertain. This uncertainty is especially crucial for transmission infrastructure, which must be routed and built well in advance of the WSP facilities it will eventually serve.

The overarching goal of probabilistic planning models must be to identify deployment strategies that are *spatially robust* to future uncertainty; for example, identification of transmission corridors that allow for potential utilization of multiple regions and WSP technologies, depending on the evolution of costs over time. This further increases the complexity of the planning problem, but such knowledge could reduce long-term financial risk for all involved and accelerate infrastructure planning and permitting. The spatial implications of uncertainty is an unexplored but clearly important area for future research.

The immediate question, however, is *not* whether (or even how) the results of this study would change with the inclusion of transmission issues; additional technical, political, or socioeconomic constraints; or different cost assumptions. Changing model inputs would undoubtedly change the output. The more important question is whether the development of high-resolution WSP data and more sophisticated modelling techniques is worthwhile. Could such efforts lead to appreciably better outcomes in terms of power system cost, pollution, and reliability?

Using the results of this study, a back-of-the-envelope estimate is that more advanced modelling efforts could save South Africa on the order of US\$100 million in 2040 compared to current planning approaches (2010 US dollars; present value at 8 per cent real discount rate). This figure is based on comparison of the default Green scenario (conventional planning) and the optimized Variation A.¹⁰ It seems likely, given the large, multi-decade investments South Africa must make, that simultaneous optimization of WSP siting, transmission build-out, and other considerations would increase the returns. It is reasonable to expect that the greater the WSP penetration and more complex the system under study, the larger the returns to high-resolution, spatiotemporal modelling.

The value of analyses that explicitly incorporate long-term spatiotemporal data will become more pronounced as the quality and resolution of WSP time series improve. This is particularly true of wind power, where small-scale orography may provide individual wind farm sites that exhibit unusual and/or useful temporal patterns. This requires high-resolution numerical weather modelling, as currently being carried out by the WASA project. That data, along with future

¹⁰ The optimized deployment pattern in Variation A reduces the cost of CO₂ abatement by US\$3.70 per tCO₂. A rough estimate of the annual savings is made by multiplying this number by the 228.7 MtCO₂ annual emissions in Variation A. Discounted from 2040 to the present at 8 per cent results in estimated annual savings of ~US\$100 million. If Variation B is instead used as the comparator, the estimated savings increase to ~US\$300 million.

characterization of South Africa's offshore wind resources, could provide even greater opportunity for spatial optimization techniques to combine sites and technologies in particularly advantageous deployment patterns.

South Africa is well-positioned to take advantage of policy guidance provided by more advanced modelling efforts. The Renewable Energy Independent Power Producer (IPP) Procurement Programme has already successfully completed two rounds of bid solicitation, approving ~2.5 GW of WSP capacity to date.¹¹ In conjunction with the Council for Scientific and Industrial Research's (CSIR) ongoing Strategic Environmental Assessment (SEA) for wind and solar PV rollout,¹² which is tasked with identifying geographic areas best suited for deployment, there are clear policy levers by which modelling results can be used to facilitate WSP project selection and siting on the ground.

With respect to longer-term planning, both the DOE (via the IRP) and Eskom (via its ongoing Strategic 2040 Transmission Network Study) are central to the prioritization of generating technologies and build-out of new transmission infrastructure. These decisions will be heavily dependent upon the expected cost and technical performance of alternative WSP deployment strategies. Selection of preferred strategies, from among the many possible, is likely prone to suboptimal outcomes in the absence of comprehensive (ideally probabilistic), spatiotemporal modelling. Given the long life-span of transmission infrastructure, the spatiotemporal variability of WSP resources, and the dependence of project developers on grid access, well-informed coordination and planning is absolutely critical to securing clean, affordable, and reliable electricity for South Africa.

South Africa is not the only country facing these issues. Over 135 countries have adopted national renewable energy targets. For larger countries, cost-effective exploitation of *domestic* WSP resources remains the immediate task. For smaller countries (and larger countries within multinational power grids), there may be excellent and unexplored opportunities to collectively harness *regional* WSP resources, reaping economic and environmental benefits while strengthening political ties with neighbours. Development of an integrated deployment and transmission plan to harness WSP resources across southern Africa, for example, could dramatically alter the economics of renewable energy in the region. Such 'game-changing' research requires detailed knowledge of the spatiotemporal properties of renewable resources over large areas. In general, the returns to spatiotemporal modelling will increase with the size of the geographic region under study.

As countries seek to transition to power systems dependent upon intermittent WSP, the tools used to understand and plan such systems must evolve accordingly. This study demonstrates that high-resolution, spatiotemporal data and associated modelling can identify WSP deployment strategies that offer significant savings over time. This does not necessarily require multi-year projects with large research teams and budgets. With sufficient support from in-country stakeholders, low-cost, open-source data and software like those used here are capable of capturing the most critical spatiotemporal dynamics. Research in this vein can help countries intelligently harness their unique WSP resources to address climate change, air pollution, and energy security in a cost-effective and reliable manner.

¹¹ See: <http://www.ipprenewables.co.za/>

¹² See: <http://www.csir.co.za/nationalwindsolarsea/>

References

- Alliance for Climate Protection (2009). Repower America. Available at: <http://www.repoweramerica.org/> (accessed January 2013).
- Ball, M., M. Wietschel, and O. Rentz (2007). 'Integration of a Hydrogen Economy into the German Energy System: An Optimising Modelling Approach'. *International Journal of Hydrogen Energy*, 32(10): 1355–68.
- Banks, D., and J. Schäffler (2007). 'A Proposed Renewable Energy Plan of Action for the Western Cape'. Technical Report. Cape Town: Western Cape Department of Environmental Affairs and Development Planning.
- De Soto, W.L. (2004). 'Improvement and Validation of a Model for Photovoltaic Array Performance'. MSc Thesis, University of Wisconsin-Madison.
- Delucchi, M.A., and M.Z. Jacobson (2011). 'Providing All Global Energy with Wind, Water, and Solar Power, Part II: Reliability, System and Transmission Costs, and Policies'. *Energy Policy*, 39(3): 1170–90.
- Diab, R. (1985). 'Contributions of Wind Power to South Africa's Energy Needs'. *South Africa Journal of Science*, 81: 460–63.
- Dobos, A.P. (2012). 'An Improved Coefficient Calculator for the California Energy Commission 6 Parameter Photovoltaic Module Model'. *Journal of Solar Energy Engineering*, 134(2).
- DOE (2011). 'Integrated Resource Plan for Electricity 2010–2030'. Pretoria: South Africa Department of Energy. March. Available at: http://www.energy.gov.za/files/irp_frame.html (accessed August 2012).
- Elhadidy, S. (2000). 'Parametric Study of Hybrid (Wind + Solar + Diesel) Power Generating Systems'. *Renewable Energy*, 21(2): 129–39.
- Eskom (2012). 'The Strategic 2040 Transmission Network Study'. Eskom presentation to GPTRC. February.
- Fishbone, L.G., and H. Abilock (1981). 'Markal, a Linear-programming Model for Energy Systems Analysis: Technical Description of the BNL Version'. *International Journal of Energy Research*, 5(4): 353–75.
- Fluri, T.P. (2009). 'The Potential of Concentrating Solar Power in South Africa'. *Energy Policy*, 37: 5075–80.
- Gilman, P., and A. Dobos (2012). 'System Advisor Model, SAM 2011.12.2: General Description'. NREL Technical Report No. TP-6A20-53437. Golden, CO: National Renewable Energy Laboratory.
- Gunturu, U.B., and C.A. Schlosser (2012). 'Characterization of Wind Power Resource in the United States'. *Atmospheric Chemistry and Physics*, 12: 9687–702.
- Hagemann, K. (2008). 'Mesoscale Wind Atlas of South Africa'. PhD Dissertation, University of Cape Town.
- Hansen, M.O. (1998). *Basic Rotor Aerodynamics Applied to Wind Turbines*. DTU-ET-NE-98-02. Inst. for Energiteknik, Danmarks Tekniske Universitet, Lyngby.
- Hasche, B., A. Keane, and M. O'Malley (2011). 'Capacity Value of Wind Power, Calculation, and Data Requirements: The Irish Power System Case'. *IEEE Transactions on Power Systems*, 26(1): 420–30.

- Hiemstra, P.H., E.J. Pebesma, C.J.W. Twenhöfel, and G.B.M. Heuvelink (2009). ‘Real-time Automatic Interpolation of Ambient Gamma Dose Rates from the Dutch Radioactivity Monitoring Network’. *Computers and Geosciences*, 35(8): 1711–21.
- Ihle, J., and B. Owens (2004). ‘Integrated Coal and Wind Power Development in the U.S. Upper Great Plains’. Platts Research and Consulting Concept Paper, February. Boulder, CO: Department of Regulatory Agencies of Colorado.
- Jacobson, M.Z., and M.A. Delucchi (2011). ‘Providing All Global Energy with Wind, Water, and Solar Power, Part I: Technologies, Energy Resources, Quantities and Areas of Infrastructure, and Materials’. *Energy Policy*, 39: 1154–69.
- Keane, A., M. Milligan, C.J. Dent, B. Hasche, C. D’Annunzio, K. Dragoon et al. (2011). ‘Capacity Value of Wind Power’. *IEEE Transactions on Power Systems*, 26(2): 564–72.
- King, D.L., S. Gonzalez, G.M. Galbraith, and W.E. Boyson (2007). ‘Performance Model for Grid-connected Photovoltaic Inverters’. Albuquerque, NM: Sandia National Laboratories.
- Lage, J.P., R.M. Assunção, and E.A. Reis (2001). ‘A Minimal Spanning Tree Algorithm Applied to Spatial Cluster Analysis’. *Electronic Notes in Discrete Mathematics*, 7: 162–65.
- Lobo, F.G., and C.F. Lima (2007). ‘Adaptive Population Sizing Schemes in Genetic Algorithms’. *Studies in Computational Intelligence*, 54: 185–204.
- Makarov, Y.V., Z. Huang, P.V. Etingov, J. Ma, R.T. Guttromson, K. Subbarao et al. (2010). ‘Incorporating Wind Generation and Load Forecast Uncertainties into Power Grid Operations’. Richland, WA: Pacific Northwest National Laboratory, U.S. Department of Energy. Available at: http://www.pnl.gov/main/publications/external/technical_reports/PNNL-19189.pdf (accessed September 2012).
- Mebane Jr, W.R., and J.S. Sekhon (2011). ‘Genetic Optimization Using Derivatives: The Rgenoud Package for R’. *Journal of Statistical Software*, 42(11): 1–26.
- Milligan, M., and K. Porter (2008). ‘Determining the Capacity Value of Wind: An Updated Survey of Methods and Implementation’. Presented at WindPower 2008, June. Available at: <http://www.nrel.gov/docs/fy08osti/43433.pdf> (accessed September 2012).
- Mueller, R., T. Behrendt, A. Hammer, and A. Kemper (2012). ‘A New Algorithm for the Satellite-based Retrieval of Solar Surface Irradiance in Spectral Bands’. *Remote Sensing*, 4(3): 622–47.
- Neises, T. (2011). ‘Development and Validation of a Model to Predict the Cell Temperature of a Photovoltaic Cell’. MSc Thesis, University of Wisconsin-Madison.
- NERC (2012). ‘2012 Long-term Reliability Assessment: Methods and Assumptions’. Atlanta, GA: North American Electricity Reliability Corporation, November. Available at: http://www.nerc.com/files/2012LTRA_PartII.pdf (accessed December 2013).
- Parsons-Brinckerhoff (2009). ‘Powering the Future: Mapping our Low-Carbon Path to 2050’. Available at: <http://www.pbpoweringthefuture.com> (accessed January 2013).
- Pelikan, M., K. Sastry, and D.E. Goldberg (2003). ‘Scalability of the Bayesian Optimization Algorithm’. *International Journal of Approximate Reasoning*, 31(3): 221–58.
- Peterson, E.L., N.G. Mortensen, L. Landberg, J. Hojstrup, and H.P. Frank (1997). ‘Wind Power Meteorology’. Roskilde: Riso National Laboratory.
- Philbrick, C.R. (2011). ‘Wind Integration and the Need for Advanced Decision Support Tools’. Power and Energy Society General Meeting, IEEE, San Diego, CA, 24–29 July, pp. 1–7.

- Posselt, R., R.W. Mueller, R. Stöckli, and J. Trentmann (2012). 'Remote Sensing of Solar Surface Radiation for Climate Monitoring—the CM-SAF Retrieval in International Comparison'. *Remote Sensing of Environment*, 118: 186–98.
- Pricewaterhouse-Coopers et al. (2010). Potsdam Institute for Climate Impact Research, International Institute for Applied Systems Analysis and the European Climate Forum (2010). '100% Renewable Electricity: A Roadmap to 2050 for Europe and North Africa'. Available at: http://www.pwcwebcast.co.uk/dpliv_mu/100_percent_renewable_electricity.pdf (accessed 7 August 2014).
- Quinlan, P.J.A. (1996). 'Time Series Modeling of Hybrid Wind Photovoltaic Diesel Power Systems'. MSc Thesis, University of Wisconsin-Madison.
- Reichling, J., and F. Kulacki (2007). 'Utility Scale Hybrid Wind–Solar Thermal Electrical Generation: A Case Study for Minnesota'. *Energy*, 33(4): 626–38.
- REN21 (2013). 'Renewables 2013 Global Status Report. Renewable Energy Policy Network for the 21st Century'. Available at: <http://www.ren21.net/REN21Activities/GlobalStatusReport.aspx>
- Rienecker, M.M., M.J. Suarez, R. Todling, J. Bacmeister, L. Takacs, H.-C. Liu et al. (2008). 'The GEOS-5 Data Assimilation System—Documentation of Versions 5.0.1, 5.1.0, and 5.2.0'. Technical Report Series on Global Modeling and Data Assimilation, Vol. 27. Greenbelt, MD: National Aeronautics and Space Administration.
- SAM (2013). 'System Advisor Model Version 2013.1.15 (SAM 2013.1.15)'. Golden, CO: National Renewable Energy Laboratory. Available at: <https://sam.nrel.gov/content/downloads> (accessed September 2013).
- Short, W., P. Sullivan, T. Mai, M. Mowers, C. Uriarte, N. Blair et al. (2011). 'Regional Energy Deployment System (ReEDS)'. NREL Technical Report No. TP-6A20-46534, December. Golden, CO: National Renewable Energy Laboratory.
- Simard, M., N. Pinto, J. Fisher, and A. Baccini (2011). 'Mapping Forest Canopy Height Globally with Spaceborne Lidar'. *Journal of Geophysical Research*, 116: G04021.
- Ummel, K. (2011). 'SEXPOT: A Spatiotemporal Linear Programming Model to Simulate Global Deployment of Renewable Power Technologies'. MSc thesis, Central European University.
- Ummel, K. (2013). 'Planning for Large-scale Wind and Solar Power in South Africa: Identifying Cost-effective Deployment Strategies Using Spatiotemporal Modeling'. Center for Global Development Working Paper 340. Available at: <http://www.cgdev.org/publication/planning-large-scale-wind-and-solar-power-south-africa-identifying-cost-effective> (accessed July 2014).
- Wagner, M.J., and P. Gilman (2011). *Technical Manual for the SAM Physical Trough Model*. NREL Technical Report No. TP-5500-51825, June. Golden, CO: National Renewable Energy Laboratory.